The Journal of Chemical Physics

Surprisal of a quantum state: Dynamics, compact representation, and coherence effects

Cite as: J. Chem. Phys. **153**, 214105 (2020); https://doi.org/10.1063/5.0030272
Submitted: 21 September 2020 . Accepted: 09 November 2020 . Published Online: 02 December 2020

K. Komarova, F. Remacle, and R. D. Levine

The Journal of Chemical Physics ARTICLE scitation.org/journal/jcp

Surprisal of a quantum state: Dynamics, compact representation, and coherence effects

Cite as: J. Chem. Phys. 153, 214105 (2020); doi: 10.1063/5.0030272
Submitted: 21 September 2020 • Accepted: 9 November 2020 •
Published Online: 2 December 2020

K. Komarova,[1,a)] F. Remacle,[1,2] and R. D. Levine[1,3]

AFFILIATIONS

[1]The Fritz Haber Center for Molecular Dynamics and Institute of Chemistry, The Hebrew University of Jerusalem, Jerusalem 91904, Israel
[2]Theoretical Physical Chemistry, UR MolSys B6c, University of Liège, B4000 Liège, Belgium
[3]Department of Chemistry and Biochemistry, University of California, Los Angeles, California 90095, USA and Department of Molecular and Medical Pharmacology, David Geffen School of Medicine, University of California, Los Angeles, California 90095, USA

[a)]**Author to whom correspondence should be addressed:** ksenia.komarova@mail.huji.ac.il

ABSTRACT

Progress toward quantum technologies continues to provide essential new insights into the microscopic dynamics of systems in phase space. This highlights coherence effects whether these are due to ultrafast lasers whose energy width spans several states all the way to the output of quantum computing. Surprisal analysis has provided seminal insights into the probability distributions of quantum systems from elementary particle and also nuclear physics through molecular reaction dynamics to system biology. It is therefore necessary to extend surprisal analysis to the full quantum regime where it characterizes not only the probabilities of states but also their coherence. In principle, this can be done by the maximal entropy formalism, but in the full quantum regime, its application is far from trivial [S. Dagan and Y. Dothan, Phys. Rev. D **26**, 248 (1982)] because an exponential function of non-commuting operators is not easily accommodated. Starting from an exact dynamical approach, we develop a description of the dynamics where the quantum mechanical surprisal, a linear combination of operators, plays a central role. We provide an explicit route to the Lagrange multipliers of the system and identify those operators that act as the dominant constraints.

I. INTRODUCTION

Quantum technologies are receiving increasing attention. This fast growing field and the outstanding experimental progress stimulate the developments of theoretical methodologies that provide a quantum approach to nano-systems. In particular, experimental techniques that can pump and probe coherence effects such as two-dimensional electronic spectroscopy have provided considerable stimulus.[1,2] We here highlight an information theory motivated[3–5] quantum dynamical approach which we implement in a numerically accurate way. Information theory, initially formulated by Shannon[6] for classical statistical ensembles, was later generalized for the case of quantum mechanical systems.[7,8] An information theoretical description of systems not in equilibrium has been examined all the way from elementary particle[9] and nuclear heavy ion physics[10] through chemical reaction dynamics[11] to gene expression levels[12,13] and cell–cell dynamics.[14] In all these implementations, large or small systems, the surprisal offers an approximate but quite compact representation. Almost invariably, in such complex systems, there is extensive summation over final quantum states. The grouping of states can be extreme as when we group together all the quantum states of a given species. The grouping of states gives rise to the concept of a prior distribution,[15,16] namely, the weights of the different groups of unresolved states. The prior distribution can be very non-uniform and a part of the variability of the observed distribution. In this paper, we discuss a fully resolved quantum state distribution.

The key feature of the present work is a quantum dynamical framework for the time evolution of the surprisal where coherence effects can be prominent. Our two examples are drawn from ultrafast

(few femtoseconds) excitation and non-adiabatic transfer processes between a pair of electronic states. The theory as we develop it here is limited to a unitary time evolution so that realistically it can only cover a finite time interval. A coupling of the system to its environment can also be described by the Lie algebraic technique that we use,[17] but such an application of the surprisal as an exact numerical tool remains to be implemented in detail.

We develop an approach where the time-evolution of a quantum system is provided through the surprisal of the density matrix, $\hat{I} = -\ln \hat{\rho}$. We specifically refer to the density matrix on the basis of individual quantum states. The practically important question of an incomplete resolution of the quantum states[15,18] will be discussed in a following publication. Here, we deal with a detailed resolution so that there is no need to introduce a prior distribution[15] or, in other words, the prior distribution is uniform. The propagation of the surprisal in time is described by the same evolution operator as the propagation of the density matrix. We also point to the connection to empirical surprisal analysis. In these practical applications, approximate compact representations of the surprisal were used to characterize the dominant behavior patterns in complex systems.[11,19]

The characterization of a system using the logarithm of its probability distribution was pioneered already by Gibbs and Boltzmann. The statistical notion of entropy was introduced by Boltzmann as a logarithmic measure of the number of states with a significant probability of being occupied. Gibbs described the properties of the canonical ensemble showing that it is characterized by the maximum of entropy. The quantum mechanical foundations of these thermodynamic ideas are given in detail in Chap. V of Ref. 20 and are discussed critically by Kemble.[21]

Already in Boltzmann's "method of the most probable distribution," one can identify the main idea that accompanied surprisal along its historical path—the idea of asking only questions about the properties of the system that are reproducible in many experimental replications. The connection to information theory can be made by special reference to the first coding theorem of Shannon.[6] The quantum mechanical analog of the coding theorem is by Schumacher.[8] It provides a basis for the quantum mechanical applications of information theory.

How can one determine the state of the system leading to events that are most probable and therefore reproducible by repeated experiments? The maximal entropy approach seeks to reconstruct the density matrix of the system in its most probable state in a situation of incomplete knowledge, when only partial information about the system is available.[3,4,7,22,23] The commonly discussed scenario is when we know N mean values for a set of operators typically called the constraints. This can be realized both for quantum and classical cases (see more detailed discussion in Sec. S3 1 of the supplementary material). In general, this set of expectation values is not sufficient to uniquely determine the state. Among all density operators that are consistent with the given mean values of the constraints, we select the one (unique) density whose entropy is maximal. This density operator is represented as an exponential function of those operators whose mean values are given. For this density matrix, the surprisal is a linear function of the operators that are the constraints. The coefficients of the constraints are the Lagrange multipliers that arise in seeking a maximum of the entropy subject to these constraints. The linearity of the surprisal as a function of the constraints is especially convenient when the operators do not commute and an exponential form in the operators calls for special handling (see, e.g., Ref. 24).

An established route for the computation of the dynamical evolution of the surprisal is via an algebraic procedure for the dynamics of the constraints in the Heisenberg picture. The equations of motion for the constraints are derived using their commutation relation with the Hamiltonian and can be solved analytically if the set of constraints is closed. This exact approach needs tracking as many constraints as the number of operators needed in a set that is closed upon the commutation with the Hamiltonian. However, often in the cases important for dynamical processes that set appears not to be finite, and therefore, the algebraic route does not provide a simple and compact representation of the surprisal as the dynamics unfold. We here examine a direct way to compute the time-evolution of the surprisal by explicit propagation on a finite, possibly large, basis set. This approach, in general, provides access to the time-dependent surprisal. It can be seen as an alternative way of computing the time-evolution of a quantum mechanical system, and as such, it may point the way to approximate the treatment of the quantum dynamics.

In this digital age, a numerical implementation of quantum mechanics often implies working with a finite, albeit possibly large, basis set. Hence, we often formulate our results below in a finite dimensional space. We point it out when we do it particularly so because when the basis set is finite, one can show that there is a large yet finite set of constraints that allow for an exact representation of the surprisal within that space. A general finite basis approach is to implement the computation of the dynamics of the wave function defined on a grid.[25–27] For a pure state, it means propagating a wave packet, the simplest case being a Gaussian.[28] A moving wave packet can describe a reactive collision when the packet initiates in the reactant region. The packet proceeds to the products region, while some of it is reflected back to the reactants (see, e.g., Ref. 27). Such a localized wave packet does not have a sharp energy. A state where several electronic states are coherently excited by an ultrafast pulse is equally not a state of sharp energy.

To represent the change of the surprisal in time, we first discuss the time rate of change of the constraints. However, in those cases, when the algebra of time-independent constraints is closed, there is a complementary view using a set of time-dependent coefficients, the Lagrange multipliers. There is a multiplier associated with each constraint, and in this point of view, it is the multiplier that is changing with time, but the constraint operators are time-independent (see Secs. II C and II D for details). Thereby, we can describe the evolution of the state by a vector of these Lagrange multipliers defined on a map of the finite set of time-independent constraints (Fig. 1).

If we keep the same algebraic structure of the dynamics, the map of the constraints stays the same and different dynamical problems can be characterized by the respective vectors of the Lagrange multipliers. This is analogous to the color palette structure: red, green, and blue primary colors of each pixel are the same, but their intensity variation enables us to create all kinds of images. We discuss the examples of the evolution of the Lagrange multipliers computed for the nuclear quantum dynamics unfolding on several electronic states coupled either by a short ultrafast pulse or by a longer lasting diabatic coupling. We extend the Lagrange

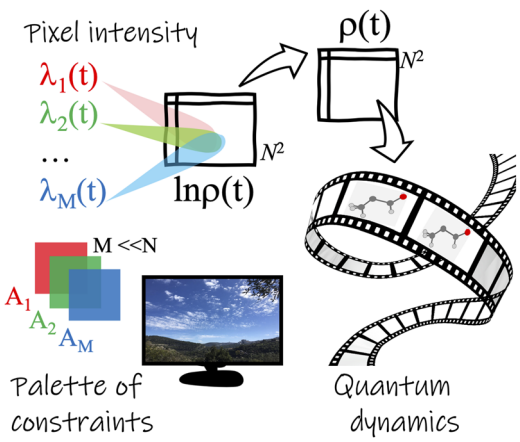

FIG. 1. Surprisal based quantum dynamics. Decomposition of the surprisal $\ln\hat{\rho}(t)$ in a finite set of time-independent constraints $\hat{A}_k$ is shown as a palette of primary colors, with the respective intensity of each color defined by its time-dependent Lagrange multiplier $\lambda_k(t)$.

multiplier formalism also for the cases when we solve numerically for the time propagation of the surprisal. In particular, we identify leading or "dominant" constraints. This approximate treatment follows the spirit of the information theory approach—a description of the density matrix using only a partial but essential knowledge about the system.

To discuss systems with more than a few degrees of freedom, a large basis is needed for numerical convergence. Hence, the exact propagation of the surprisal on a finite basis will be computationally demanding. However, the dynamics of the Lagrange multipliers of the dominant constraints may be sufficient for most purposes. This opens a different way of approximating the quantum dynamics in many-body systems, a subject for future research.

In Sec. II, we show that if the initial state of a system is described as a state of maximal entropy, a finite set of time-dependent constraints is sufficient to reproduce the surprisal at all subsequent times. During a unitary time-evolution, the rank of the density matrix is conserved so the number of the time-dependent constraints is the same as the number of constraints on the initial state. In Sec. II, we further describe the special circumstances where an algebraically delineated finite set of time-independent constraints is sufficient to describe the dynamics. The algebraic procedure to convert the dynamics of the surprisal to a compact evolution of the Lagrange multipliers is introduced. Section III discusses the proposed computational scheme for an exact dynamical evolution of the surprisal in a finite dimensional space. The computation of the time evolution in such a space is exact because we show that there is always a large but finite set of time-independent constraints that is closed under commutation with the Hamiltonian. There is however a truncation error associated with the use of a space of finite dimensions, and one should verify convergence meaning that the number of basis states is large enough. In Sec. III, we also seek to identify a much smaller set of "dominant" constraints that allow a good approximation for the state. The procedures for the computation of the surprisal and of the Lagrange multipliers are implemented in Sec. IV. We discuss three cases. The simplest is where we are able to generate a set of operators that is closed under commutation with the Hamiltonian. We next examine a case of more realistic Hamiltonian where we are not able to close a set. We take a commutator of an operator in the set with the Hamiltonian, and it can be shown that a new operator not yet in the set emerges, and so on. In this case, we can propagate the surprisal on a finite basis and numerically determine the Lagrange multipliers for operators of interest. This allows us to get an approximate description of the surprisal as a function of a finite set of operators also when their algebra is not closed. The third case we discuss is non-adiabatic transfer from an excited electronic state to a lower manifold. Here too, the algebra is not closed, but a realistic approximation for the surprisal in a limited set of constraints can be generated.

II. THE DENSITY MATRIX AND THE SURPRISAL: A GENERAL OVERVIEW

A. Finite matrix representation for the density operator and its surprisal

A simple and familiar state of maximal entropy is the density operator of a thermal state $\hat{\rho} = Z^{-1}\exp\{-\beta\hat{H}_0\}$ for a model Hamiltonian, $\hat{H}_0$, with a known basis set so that one can represent the density and the surprisal, $\hat{I}$, using a finite number, N, of states,

$$\begin{aligned}\hat{\rho} &= Z^{-1}\sum_{s=0}^{N}\exp(-\beta\varepsilon_s)|s\rangle\langle s|,\\ \hat{I} &= -\ln\hat{\rho} = \ln Z + \beta\sum_{s=0}^{N}\varepsilon_s|s\rangle\langle s|,\end{aligned} \tag{1}$$

where $\{\varepsilon_s, |s\rangle\}$ are the eigenvalues and eigenvectors of the Hamiltonian $\hat{H}_0$, respectively, $\beta = (kT)^{-1}$ is the inverse temperature, and $Z = \sum_{s=0}^{N}\exp(-\beta\varepsilon_s)$ is the partition function. In case that the eigenenergies are degenerate, each eigenstate is included separately, and there is no grouping of eigenstates. The truncation to a finite basis assumes that the eigenvalues of the Hamiltonian are ordered so that from a certain value of N and on, it is the case that $\boldsymbol{\beta}\ \varepsilon_N \gg 1$. As is well known, a finite spectral expansion is the best approximation for the density matrix in the sense of a minimal norm of the error squared.[29] For such values of the temperature that $\boldsymbol{\beta}\ \boldsymbol{\varepsilon}_s \gg 1$, $s < N$, the numerical rank of the density matrix is lower than N. At a sufficiently high $\boldsymbol{\beta}$, low temperature, and assuming a finite gap between a non-degenerate ground (GS) and a lowest excited state (ES), one can reduce the numerical rank toward unity. In this limit, the density tends to that of a pure (ground) state. At a low rank, it is numerically not practical to go from the density to its surprisal. The other direction, to determine the density from its surprisal, is possible at all temperatures.

The eigenstates that diagonalize the density matrix will also diagonalize the matrix of the surprisal. This enables a simple transformation of the time-dependent surprisal to the density matrix. When it is a thermal initial state, the eigenstates at the initial time correspond to the eigenstates of the unperturbed Hamiltonian $\hat{H}_0$. As the dynamics unfolds, the eigenstates need to be determined by diagonalization of the surprisal. In this paper, we assume that the

system is isolated in the sense that it is not interacting with its environment. The time evolution of the density is then unitary, its rank is preserved in time, and using the time-evolution operator U, the evolution of the density can be described by the evolution of each eigenstate,

$$\hat{\rho}(t) = \hat{U}\hat{\rho}_0\hat{U}^\dagger = Z^{-1}\sum_{s=0}^{N}\exp(-\beta\varepsilon_s)\left(\hat{U}|s\rangle\right)\left(\langle s|\hat{U}^\dagger\right)$$
$$= Z^{-1}\sum_{s=0}^{N}\exp(-\beta\varepsilon_s)|s(t)\rangle\langle s(t)|. \quad (2)$$

The higher the numerical rank of the initial state, the more eigenstates need to be computed for such an expansion. Therefore, an eigenstate propagation is numerically not an optimal approach for an initial density that represents a highly mixed state.

Several key features of the representation of the density matrix in Eq. (2) are, in fact, much more general that the derivation based on a thermal-like initial density would suggest. The detailed discussion is the subject of Sec. III where we will suggest that in a finite basis, as in Eq. (1), the most general form of the density matrix is

$$\hat{\rho}(t) = Z^{-1}\sum_{s=0}^{N}\exp(-\mu_s)|s(t)\rangle\langle s(t)|, \quad (3)$$

where the eigenvalues of the surprisal $\boldsymbol{\mu_s}$ are time-independent with values determined by the initial state $\boldsymbol{\rho}(t=0)$. The partition function Z is, as in Eq. (1), $Z = \sum_{s=0}^{N}\exp(-\mu_s)$. The eigenstates $|s(t)\rangle$ in Eq. (3) are, like in Eq. (2), obtained by the time-dependent propagation of the eigenvectors of the initial density. In a thermodynamic analogy,[30] the chemical potential of state s is $\ln Z + \boldsymbol{\mu_s}$ and the more negative it is, the higher is the occupancy of the state.

B. Expansion of the surprisal via a finite set of constraints

We discuss three different motivations for representing the density as an exponential function of a sum of operators and determine a condition under which the three representations are equivalent and when they are dynamically exact. The simplest to state is an inference of the density matrix at time t by the maximum entropy formalism.[3,4,7] We seek the density that is of maximal entropy given the constraint that the density is normalized and is consistent with the mean values $\langle\hat{A}_k\rangle(t) \equiv Tr\left(\hat{A}_k\boldsymbol{\rho}(t)\right)$ of Hermitian observables $\hat{A}_k$ indexed by k. It is convenient to include a $k=0$ term as the condition of normalization, $\hat{A}_0 = \hat{\mathbb{I}}$ or $Tr(\boldsymbol{\rho}(t)) = 1$. In the specific example of a thermal state, the mean energy of the system, $\langle H_0\rangle$, plays a role of the only constraint, besides normalization. Motivated by the empirical results of surprisal analysis,[11,19] we want to describe a more general case, which leads to the expression for the density of maximal entropy at the time t for which the mean values are given,

$$\boldsymbol{\rho}(t) = \exp(-\sum_{k=0}\boldsymbol{\lambda}_k(t)\hat{A}_k). \quad (4)$$

The coefficients $\boldsymbol{\lambda}_k(t)$, $k = 0, 1, \ldots$ are the Lagrange multipliers that are the variational parameters that arise in seeking the maximum of the entropy of the density subject to the imposed constraints. The Lagrange multipliers are time-dependent if the mean values $\langle\hat{A}_k\rangle(t)$ assume different values for different times. In the classical limit, the constraints are functions defined over the phase space.

We next consider two other derivations of a density matrix that are also of an exponential form like Eq. (4) but where the motivation is tightly connected to the dynamics. In a theoretical or computational discussion, one often initiates the dynamics from a pure state. However, in reality, the initial state is often a mixture, and then, it makes sense to start from an initial density of maximal entropy subject to those constraints that govern the yet unperturbed state, $\boldsymbol{\rho}(t=0) = \exp(-\sum_k\boldsymbol{\lambda}_k(t=0)\hat{A}_k)$. For such an initial state, we now show that the exact time evolution of the density or of the surprisal is described with a finite number of time-dependent constraints with time-independent Lagrange multipliers. The proof requires the unitarity of the time-evolution operator $U(t)$ and a series expansion of the exponential,

$$\boldsymbol{\rho}(t) = U(t)\boldsymbol{\rho}(t=0)U^\dagger(t)$$
$$= \exp\left(-\sum_k\boldsymbol{\lambda}_k(t=0)\left\{U(t)\hat{A}_kU^\dagger(t)\right\}\right). \quad (5)$$

The time-dependent constraints are the terms in the curly brackets, $\left\{U(t)\hat{A}_kU^\dagger(t)\right\}$, and there are as many time-dependent constraints as the number of constraints in the initial state. In Sec. III, we discuss how to compute directly the surprisal,

$$\hat{I}(t) = -\hat{U}(t)\ln\hat{\rho}(t=0)\hat{U}^\dagger(t)$$
$$= -\sum_k\lambda_k(t=0)\left\{\hat{U}(t)\hat{A}_k\hat{U}^\dagger(t)\right\}. \quad (6)$$

The method of computing the surprisal can also be applied should we wish to obtain explicit expressions for the individual time-dependent constraints.

We next come to a simpler but more specialized result. It is valid for the special case when the dynamics of the constraints are closed under commutation relation with the Hamiltonian. In such a limiting situation, the exact time evolution can be described with a finite number of time-independent constraints but with time-dependent Lagrange multipliers with known equations of motion. This third example of an exponential form for the density is the most straightforward of all three and deserves its own subsection, Secs. II C–II D. This approach that is exact is also the basis for more approximate but numerically accurate approximations that we will present.

C. Expansion of the surprisal via a finite set of constraints: A closed algebra

We now examine the special case when the exact time-evolution of the surprisal can be written as

$$\hat{I}(t) = \sum_k\lambda_k(t)\hat{A}_k \quad (7)$$

with time-independent operators and time-dependent Lagrange multipliers. For a unitary time-evolution, the equation of motion of any function of the state $\hat{\boldsymbol{\rho}}(t)$ is to be computed via the Liouville equations of motion. In particular for the surprisal written as above,

$$\frac{d\hat{I}}{dt} = -\frac{i}{\hbar}[\hat{H},\hat{I}] = -\frac{i}{\hbar}\sum_k \lambda_k(t)[\hat{H},\hat{A}_k], \tag{8}$$

where $\hat{H}$ is the Hamiltonian that defines the unitary time-evolution, $\hat{U} = \exp(-(i/\hbar)\hat{H}t)$.

The special case when the algebra is closed under commutation with the Hamiltonian is defined by the relation

$$-\frac{i}{\hbar}[\hat{H},\hat{A}_k] = \sum_s g_{ks}\hat{A}_s. \tag{9}$$

Each commutator on a right-hand side of Eq. (8) results in a linear combination of operators that constitute our closed set of constraints, as shown in Eq. (9). The numerical coefficients g_{ks} are determined by the algebra of the particular system with several examples worked out in Sec. IV. Several other, different, examples were recently published[31] in connection with quantum computing. For earlier and simpler examples, see Ref. 32. By combining Eqs. (8) and (9), we have two expressions for the equation of motion of the surprisal, where either is linear in the constraints,

$$\begin{aligned}\frac{d\hat{I}}{dt} = -\frac{i}{\hbar}[\hat{H},\hat{I}] &= -\frac{i}{\hbar}\sum_k \lambda_k(t)[\hat{H},\hat{A}_k] \\ &= \sum_{k,s}\lambda_k(t) g_{ks}\hat{A}_s \\ &= \sum_k \frac{d\lambda_k(t)}{dt}\hat{A}_k.\end{aligned} \tag{10}$$

The g_{ks} is the coefficient of the operator $\hat{A}_s$ in the commutator $-(i/\hbar)[\hat{H},\hat{A}_k]$, following Eq. (9). In Eq. (10), the unknowns are the functions of time, the Lagrange multipliers $\lambda_k(t)$.

D. Equations of motion for the Lagrange multipliers

To derive the equations of motion for the Lagrange multipliers that are associated with N constraints, we impose an orthogonality of the constraints in the $\{|n\rangle\}_{n=0,\ldots,M}$ finite basis representation. In order to solve Eq. (10), in general, we define the orthogonality of the operators from the set via the Hilbert–Schmidt inner product,[33]

$$\begin{aligned}(\hat{A}_k,\hat{A}_l) = Tr(\hat{A}_k^\dagger\hat{A}_l) &= \sum_{n=0}^{M}\langle n|\hat{A}_k^\dagger\hat{A}_l|n\rangle \\ &= \sum_{n=0}^{M}\sum_{m=0}^{M}\langle n|\hat{A}_k^\dagger|m\rangle\langle m|\hat{A}_l|n\rangle.\end{aligned} \tag{11}$$

Note that no information about the density of the system is involved here, and therefore, these inner products need to be computed only once for a selected set of time-independent constraints, so it can be done ahead of time. Knowing the matrix representation of each constraint in the chosen finite basis, we evaluate these traces for all pairs of operators in the set. We next form an "overlap" matrix for the set of constraints [see Eq. (11) and the detailed discussion in Sec. S1 of the supplementary material]. To obtain an orthogonal set of operators, as discussed in detail in Sec. S1 of the supplementary material, we diagonalize this overlap matrix and transform to a new set of constraints that satisfies the orthogonality condition,

$$(\hat{B}_k,\hat{B}_l) = \mathrm{Tr}(\hat{B}_k^\dagger\hat{B}_l) = \sum_n \langle n|\hat{B}_k^\dagger\hat{B}_l|n\rangle = F_k\delta_{kl}. \tag{12}$$

Here, $F_l = \mathrm{Tr}(\hat{B}_l^\dagger\hat{B}_l)$ is an eigenvalue of the overlap matrix. Note that this orthogonalization is time-independent and will be valid all the times of the dynamics.

The transformation matrix computed from the diagonalization allows us to rewrite the initial set of constraints using the orthogonal set $\{\hat{B}_q\}$, $q = 0,\ldots,N$,

$$\hat{A}_k = \sum_{q=0}^{N} a_{kq}\hat{B}_q. \tag{13}$$

As the transformation (13) is linear, it cannot affect the closure of the algebra; therefore, we can describe the surprisal using this orthogonal set of constraints following the same development as in Eqs. (7)–(10),

$$\begin{aligned}\frac{d\hat{I}}{dt} = \frac{d}{dt}\left(\sum_q \lambda_q(t)\hat{B}_q\right) &= \sum_q \frac{d\lambda_q(t)}{dt}\hat{B}_q \\ &= \sum_{q,s}\lambda_q(t)\tilde{g}_{qs}\hat{B}_q.\end{aligned} \tag{14}$$

Here, the coefficients $\tilde{g}_{qs}$ are obtained by considering the commutation relations $-(i/\hbar)[\hat{H},\hat{B}_q] = \sum_s \tilde{g}_{qs}\hat{B}_s$. By multiplying both sides of Eq. (14) from the left by the operator $\hat{B}_p^\dagger$, computing the trace, and dividing by the respective F_p, we get

$$\begin{aligned}\frac{1}{F_p}\mathrm{Tr}\left(\hat{B}_p^\dagger\cdot\frac{d\hat{I}}{dt}\right) &= \frac{1}{F_p}\sum_q \frac{d\lambda_q(t)}{dt}\mathrm{Tr}\left(\hat{B}_p^\dagger\cdot\hat{B}_q\right) \\ &= \frac{1}{F_p}\sum_{q,s}\lambda_q(t)\tilde{g}_{qs}\,\mathrm{Tr}\left(\hat{B}_p^\dagger\cdot\hat{B}_s\right),\end{aligned} \tag{15}$$

$$\frac{d\lambda_p(t)}{dt} = \sum_q \lambda_q(t)\tilde{g}_{qp}. \tag{16}$$

Equations of motion (16) allow propagating the set of Lagrange multipliers and therefore convert the information about the time-evolution of the $N+1$ by $N+1$ surprisal matrix to an equation of motion of a vector of at most $N+1$ components, the time-dependent Lagrange multipliers. As shown above, this reduction is only possible subject to a set of constraints and Hamiltonian that satisfy the closure relation, Eq. (9). It is often the case that to have a closed set, one needs to augment the set of constraints that specify the initial state. As a practical aspect, this means that when solving the equation of motion (16), the Lagrange multipliers for those constraints that are not needed to specify the initial state have the initial condition $\lambda_q(t=0) = 0$. In Sec. III, we discuss a more general solution valid for any initial state and unitary dynamics while keeping the limitations that we work in a finite dimensional space.

III. EXACT QUANTUM DYNAMICS OF THE SURPRISAL IN A MATRIX FORM

A. The matrix time-dependent surprisal

This section establishes a general computational procedure for determining the time evolution of the surprisal and, if needed, of the Lagrange multipliers also for such cases when the set of constraints is not an algebra closed under commutation with the Hamiltonian.

The promise of the direct surprisal propagation as opposed to the propagation of wave functions in a finite representation is primarily connected to the possibility of compressing the information about the dynamics into a vector of Lagrange multipliers of significantly lower dimensionality. This compaction is most advantageous for a mixed initial state when, in a wave function approach, one will need to time propagate as many different wave functions as the rank of the initial state.

1. Initial conditions

For an initial state of maximal entropy, an analytical expression of the surprisal as a function of a finite set of operators enables the evaluation of the matrix representation of the surprisal of the initial state in any suitable finite basis,

$$I_{ij}(t=0) = \langle i|\sum_k \lambda_k(t=0)\hat{A}_k|j\rangle = \sum_k \lambda_k(t=0)A_k^{ij}. \tag{17}$$

Here, $A_k^{ij} = \langle i|\hat{A}_k|j\rangle$ is the ij-matrix element of the constraint operator $\hat{A}_k$ in the chosen basis. When it is the initial density matrix that is given, one can get the initial form of the surprisal matrix, limited to the numerical rank of the initial density matrix.

2. Equations of motion

Given the representation of the surprisal as an N by N matrix in a finite basis,

$$\hat{I}(t) = -\ln\hat{\rho}(t) = \sum_{n,m=1}^{N} |n\rangle I_{nm}(t)\langle m|, \tag{18}$$

the time-dependence of the matrix elements $I_{nm}(t)$ can be computed from the *closed* set of N by N first order linear equations of motion for the surprisal,

$$\frac{dI_{qs}}{dt} = \frac{i}{\hbar}\sum_{m=1}^{N} I_{qm}H_{ms} - \frac{i}{\hbar}\sum_{n=1}^{N} H_{qn}I_{ns}. \tag{19}$$

Here, $\hat{H}_{ij}$ are matrix elements of the Hamiltonian $\hat{H}$ in the finite basis. In a matrix form, Eq. (19) is simply the commutation of the surprisal and the Hamiltonian matrices,

$$-i\hbar d\mathbf{I}/dt = (\mathbf{I}\cdot\mathbf{H} - \mathbf{H}\cdot\mathbf{I}). \tag{20}$$

Using the matrix of the surprisal at each time step of the dynamics, one can determine and analyze the density.

As a practical matter and in the examples discussed in Sec. IV, we define the density by first diagonalizing the surprisal and then using the spectral representation,

$$\begin{aligned} -\ln\hat{\rho}(t) &= \sum_s \mu_s|s(t)\rangle\langle s(t)|, \\ \hat{\rho}(t) &= \sum_s \exp(-\mu_s)|s(t)\rangle\langle s(t)|. \end{aligned} \tag{21}$$

Here, $|s(t)\rangle$ are the time-dependent eigenvectors with the respective time-independent eigenvalues μ_s. The decomposition of the eigenvectors of the surprisal in terms of the states of the finite basis, $|s(t)\rangle = \sum_i b_{is}(t)|i\rangle$, enables the computation of those mean values of interest using the trace of the respective operator with the density,

$$\langle\hat{O}\rangle(t) = \mathrm{Tr}(\hat{\rho}(t)\hat{O}) = \sum_s \exp(-\mu_s)\sum_{i,j} b_{js}^*(t)O_{ji}b_{is}(t). \tag{22}$$

3. The Gelfand basis

A basis set for the operators represented as N by N matrices is the, so called, Gelfand matrices,[34,35] $\mathbf{E}_{nm}$, where each is a matrix of zeros except for the entry 1 at the intersection of row n and column m. For the N by N surprisal matrix, we can write an exact expansion in the N^2 matrices of the Gelfand basis $\boldsymbol{I}(t) = \sum_{n,m=1}^{N} I_{nm}(t)\mathbf{E}_{nm}$. This is the matrix form of Eq. (18). One can regard this necessarily exact expression in an N by N basis as a result of maximal entropy subject to the N^2 constraints $\langle\mathbf{E}_{nm}\rangle$ with the $I_{nm}(t)$ as their conjugate Lagrange multipliers. Of course, speaking from a parsimonious point of view, this can be many more constraints than are strictly needed, but maximal entropy subject to more than the minimal number of valid constraints does yield correct results.

The representation of the surprisal matrix $\mathbf{I}(t) = \sum_{n,m=1}^{N} I_{nm}(t)\mathbf{E}_{nm}$ uses, as in other examples above, time-independent constraints and their time-dependent Lagrange multipliers. The set of constraints is closed because the Gelfand states are closed under commutation among themselves, $[\mathbf{E}_{mn}, \mathbf{E}_{kl}] = \mathbf{E}_{ml}\delta_{nk} - \mathbf{E}_{kn}\boldsymbol{\delta}_{lm}$ and any N by N matrix, including the Hamiltonian, can be written as a linear combination of the Gelfand basis matrices. What are the basis states is a matter of convenience. It can be a set of zero order wave functions or it can be points in a discrete grid. The essential point is that the basis needs to be large enough that the initial states and their subsequent evolution can be numerically closely approximated.

4. A pure state

A closed algebra of the constraints is defined by Eq. (9). Taking the expectation value of both sides leads to a closed set of equations of motion for the mean values of the constraints,

$$\frac{d\langle\hat{A}_k\rangle(t)}{dt} = \frac{i}{\hbar}\langle[\hat{H},\hat{A}_k]\rangle = -\sum_s g_{ks}\langle\hat{A}_s\rangle(t). \tag{23}$$

The structure of this equation is the same whether the expectation value is taken over a pure or a mixed state. The essential difference is that for a mixed state, this can be an equation for a set of mean values that is sufficient to fully specify the state. For a pure state, these expectation values are not necessarily sufficient. There can be density matrices of finite entropy that are consistent with the given expectation values. It then takes additional expectation values to reduce the maximal value of the entropy toward zero. However, as a practical matter, these finite number of equations can be sufficient for an excellent numerical approximation. This will be particularly so when the operators and the density are expressed as matrices in a finite but sufficiently large basis. When we work in a finite basis in the limiting case of a pure state, a diagonalized surprisal matrix will have only one eigenvector with an eigenvalue close to zero, and the other eigenvalues being larger negative numbers. The density matrix [cf. Eq. (21)] will then have a one dominant eigenvector

with an eigenvalue rather close to unity up to the desired numerical precision with other eigenvectors having exponentially smaller eigenvalues.

B. The general procedure to determine the Lagrange multipliers

The values of the Lagrange multipliers can be determined from the matrix representation of the surprisal following a similar procedure as in Eq. (15),

$$\lambda_p(t) = \frac{1}{F_p}\mathrm{Tr}\left(\hat{B}_p^\dagger \cdot \hat{I}(t)\right) = \frac{1}{F_p}\sum_{i,j}\langle i|\hat{B}_p^\dagger|j\rangle \cdot I_{ji}(t). \tag{24}$$

Here, we used the orthogonality of the constraints $\{\hat{B}_q\}$ as described by Eq. (12). The finite basis representation is not arbitrary, it should be the same as the representation of the surprisal. Equation (24) is our central result for computing the Lagrange multiplier conjugate to any operator. The condition on the operator to have a non-zero Lagrange multiplier is that it is not orthogonal, in the sense of a Hilbert–Schmidt norm, to the surprisal at that point in time.

Empirically, one finds that in surprisal analysis, a few constraints are dominant in magnitude, while others are small and often are within the experimental noise level. Here, the entropy provides a natural measure of the importance of a constraint. The constraint $\hat{B}_p(t)$ contributes to the entropy the term $\boldsymbol{\lambda}_p(t)\langle\hat{B}_p\rangle(t)$. The constraint $\hat{B}_p(t)$ is a dominant one when its contribution to the total is large. In our experience,[13] different constraints can be dominant in different time intervals.

In summary, by working in a finite basis of N states, one can compute the surprisal as an N by N Hermitian matrix that is a function of time. The one (fairly weak) requirement is that the surprisal of the initial state can be well approximated as a matrix in this basis. It requires that the initial state has a numerical rank of N or less. There is no assumption needed that we know the constraints on the initial state. If the initial state can be represented as a state of maximal entropy, we have the clear advantage that we can then determine the constraints as a function of time. Note that this does not require a closed algebra. The matrix representation is readily adapted to describing the time-dependent constraints, $U(t)\hat{A}_k U^\dagger(t)$, Eq. (5). The matrix representation of each one of these operators satisfies an equation like Eq. (20). The $\hat{\mathbf{H}}$ matrix that generates the motion in time is the same for all these operators.

We validate the implementation of the propagation of the surprisal in the matrix representation Eq. (19) and Lagrange multipliers defined by Eq. (24) via comparison with the surprisal obtained using propagation of the equations of motion for the Lagrange multipliers, Eq. (16). As we start with a pure initial state, we also perform an additional benchmark by comparison of the resulting densities and the time-dependent mean values with those calculated from the propagation of the wave function on a grid of the nuclear coordinates.

C. Summary of computational approaches

Given the matrix of the surprisal as a function of time, one computes the Lagrange multiplier conjugate to the constraint by Eq. (24). Here, $F_p = \mathrm{Tr}(\hat{B}_p^\dagger \hat{B}_p) = \sum_{nm}\left|\langle n|\hat{B}_p|m\rangle\right|^2$ is the Hilbert Schmidt norm of the constraint $\hat{B}_p$, Eq. (12) computed in the same, time-independent basis, used to represent the surprisal as a matrix. In the special case that a closed algebra is known, one can propagate the Lagrange multipliers directly in time as in Eq. (16) without the need to generate the surprisal. In this special case, the surprisal is given in terms of the Lagrange multipliers [Eq. (14)] $\hat{I}(t) = \sum_p \lambda_p(t)\hat{B}_p$. Diagonalizing the matrix of the surprisal also enables a diagonal matrix representation of the density matrix and thereby the computation of the mean values of other operators of interest.

IV. RESULTS AND DISCUSSION

In this section, we examine numerically the dynamics for a case of two coupled electronic states. The potential for the nuclear motion in either electronic state is harmonic. We discuss three cases for the coupling. (i) A short laser pulse with a constant transition dipole moment, independent of the displacement of the nuclei in the electronic states. We chose this simple case because one can readily close an algebra. (ii) The same short laser pulse with a transition dipole moment that varies linearly with the displacement of the vibrations from their equilibrium position. Here, an algebra is not closed, but the closed algebra of case (i) is dominant. (iii) The two electronic states are diabatically coupled, and we monitor the population exchange between the two states in time. This system is a simplified model of a radiationless transition, and we use potentials and couplings adapted from a study of pyrazine.[36] In the examples, the surprisal is propagated according to Eq. (19) starting from an initially non-stationary state. We use the finite basis of zero-order states—vibrational eigenstates of the harmonic potentials. The basis used is large enough that the computation is numerically accurate as shown by comparison with the benchmark results of the wave function propagation on a dense grid in the nuclear coordinate. This surprisal propagation provides the "exact" reference. The expression for the surprisal is transformed to the expression for the density via Eq. (21); thereby, the expectation values of observables, such as evolution of the population, coherence, and other mean values can be computed. We benchmark the computational scheme for the evaluation of the Lagrange multipliers, Eq. (24), by comparison with the surprisal obtained from its expansion in terms of time-independent constraints, $\hat{I}(t) = \sum_p \lambda_p(t)\hat{B}_p$. In case (i), the algebra of the constraints is closed and we propagate λ_p's directly using the equations of motion, Eq. (16). When the algebra is not closed, we determine the time dependence of the Lagrange multipliers from the general result, Eq. (24). Different approximations to the surprisal are then obtained depending on which operators $\hat{B}_p$ are kept in the expansion $\hat{I}(t) = \sum_p \lambda_p(t)\hat{B}_p$. We show the results for the smallest possible closed set of operators where already one obtains physically realistic results, the next larger algebra where the results are accurate to graph plotting accuracy and an even larger algebra where the convergence is rather acceptable.

We examine the accuracy of the presented approach on the effects of the coherence between the vibrational and electronic states for two qualitatively different initial pure states: (a) a coherent superposition of a very few vibrational states with the main population in the $v = 0$ state and (b) a coherent superposition of a larger number of excited vibrational states centered about $v = 5$. In Sec. IV A,

we present also the second set of computations, where we use the same two initial vibrational states but for a case when the transition dipole varies with the nuclear displacement. This represents the case when the algebra is not closed. Even so, we can identify a few dominant constraints. In Sec. IV B, we discuss the dynamics of ongoing population exchange between two electronic states that are diabatically coupled using a potential that varies linearly with the displacement from equilibrium. The algebra is not closed, and yet, the dominant constraints capture the dynamics in a quite realistic manner.

A. Field induced vibronic dynamics for two electronic states

1. Closed algebra for electron-nuclear dynamics

The simple case of a closed algebra is mostly to introduce ideas and notation. That there need to be prefect agreement between the exact computation and the finite sum representation of the surprisal, $\hat{I}(t) = \sum_p \lambda_p(t)\hat{B}_p$, is guaranteed. Hence, the full discussion is presented in Sec. S3 of the supplementary material. Here is only an outline.

Hamiltonian. We work in a direct product Hilbert space for electron and nuclear degrees of freedom. The Hamiltonian, including the interaction with a laser pulse $E(t)$, for the two electronic states can be written as follows (in atomic units, $\hbar = 1$):

$$\begin{aligned}\hat{H} &= \hat{H}_0 + \hat{V}(t),\\ \hat{H}_0 &= \hbar\omega \cdot \widehat{\mathbb{I}}_e \otimes \left(\hat{a}^\dagger\hat{a} + \frac{1}{2}\right) + V_0 \cdot \hat{\sigma}_z \otimes \widehat{\mathbb{I}}_N,\\ \hat{V}(t) &= -E(t)\mu\hat{\sigma}_x \otimes \widehat{\mathbb{I}}_N.\end{aligned} \tag{25}$$

Here, the operators $\widehat{\mathbb{I}}_e$ and $\widehat{\mathbb{I}}_N$ are identity operators defined on the electron and nuclear subspaces, respectively. The nuclear subspace is represented using the algebra of the creation and annihilation operators, $\{\widehat{\mathbb{I}}_N, \hat{a}, \hat{a}^\dagger, \hat{a}^\dagger\hat{a}\}$, which gives a simple Hamiltonian matrix on a finite basis of vibrational eigenstates of $\hat{H}_0$, Eq. (25). Both potentials have the common frequency ω and equilibrium position centered at $R_{eq} = 0$. The gap between the electronic states, V_0, is reflected by the operator $\hat{\sigma}_z \otimes \widehat{\mathbb{I}}_N$, and the dipole coupling to the field $\mu E(t)$ is described by $\hat{\sigma}_x \otimes \widehat{\mathbb{I}}_N$, where $\{\hat{\sigma}_x, \hat{\sigma}_y, \hat{\sigma}_z\}$ are the standard Pauli matrices used to describe the electronic subspace. The transition dipole moment $\boldsymbol{\mu}$ is here a constant, but in case (ii), it will be allowed to depend linearly on the displacement, $\hat{\boldsymbol{\mu}} = \boldsymbol{\mu}_0 + \boldsymbol{\mu}_1(\hat{a}^\dagger + \hat{a})$, in which case, the algebra is not closed. In the bra-ket notation for the electronic states, the Hamiltonian can be written as follows:

$$\begin{aligned}\hat{H}_0 &= E_1|1\rangle\langle 1| + E_2|2\rangle\langle 2| + \hbar\omega|1\rangle\hat{a}^\dagger\hat{a}\langle 1| + \hbar\omega|2\rangle\hat{a}^\dagger\hat{a}\langle 2|,\\ \hat{V}(t) &= -E(t)\mu_0(|1\rangle\langle 2| + |2\rangle\langle 1|)\\ &\quad -E(t)\mu_1\Big(|1\rangle(\hat{a} + \hat{a}^\dagger)\langle 2| + |2\rangle(\hat{a} + \hat{a}^\dagger)\langle 1|\Big),\end{aligned} \tag{26}$$

$$E_1 = -\frac{1}{2}V_0 + \frac{1}{2}\hbar\omega \quad E_2 = \frac{1}{2}V_0 + \frac{1}{2}\hbar\omega,$$

where $|1\rangle$ and $|2\rangle$ are the electronic wave functions for the ground and excited state, respectively.

Initial conditions. We start from the initial state of maximal entropy. As we discussed above, the most simple example of such a state is the thermal state of the unperturbed Hamiltonian, Eq. (1). This is a stationary state of the Hamiltonian $\hat{H}_0$. In order to have more interesting features in the dynamics, we introduce a non-stationary initial state by shifting the initial wave packet to the extent $\boldsymbol{\delta}$ from the equilibrium position while keeping the mean momentum at zero. In addition, for such a shifted initial state, the algebra remains closed. For technical details, see Sec. S3 of the supplementary material.

The initial surprisal is given for the closed set of constraints by

$$\begin{aligned}\hat{I}(0) = -\ln\hat{\rho}(0) = {}& \lambda_0^{11}(0)|1\rangle\widehat{\mathbb{I}}_N\langle 1| + \lambda_1^{11}(0)|1\rangle\hat{a}\langle 1|\\ &+\lambda_2^{11}(0)|1\rangle\hat{a}^\dagger\langle 1| + \lambda_3^{11}(0)|1\rangle\hat{a}^\dagger\hat{a}\langle 1|\\ &+\lambda_0^{22}(0)|2\rangle\widehat{\mathbb{I}}_N\langle 2| + \lambda_1^{22}(0)|2\rangle\hat{a}\langle 2|\\ &+\lambda_2^{22}(0)|2\rangle\hat{a}^\dagger\langle 2| + \lambda_3^{22}(0)|2\rangle\hat{a}^\dagger\hat{a}\langle 2|.\end{aligned} \tag{27}$$

Here, $\lambda_k^{ij}(0)$ is an initial value of the Lagrange multiplier of the kth constraint $|i\rangle\hat{A}_k\langle j|$ defined in the direct product of the electron and nuclear subspaces and listed in Table I.

The time-evolution of the constraints is given by the commutation relations with the Hamiltonian. These are evaluated in Sec. S3 1 of the supplementary material. It shows that the equations of motion involve only the operators from the set (see Table I) so that the algebra is closed.

Orthogonalization of the constraints. To determine how the Lagrange multipliers change with time as the dynamics unfold, it is convenient to orthogonalize the operators from the set (see Table I) in the sense of Eq. (12). The electronic subspace is initially orthogonal, but we need to specifically discuss the nuclear subspace. For this set of operators, the vibrational basis of the eigenstates of $\hat{H}_0$ is most useful: the number operator $\hat{a}^\dagger\hat{a}$ is diagonal, while the creation and annihilation operators are off-diagonal in this basis, so they are orthogonal to each other (see Sec. S1 of the supplementary material for details). The identity operator $\widehat{\mathbb{I}}_N$ is also diagonal, and hence, it will not be orthogonal to the number operator. We handle this aspect as discussed in Sec. S1 of the supplementary material.

Coupled electron-nuclear dynamics. The Hamiltonian, Eq. (25), admits of a closed algebra for the operators listed in Table I. One can therefore compute numerically exact dynamics using either route,

TABLE I. Full set of operators and notations for their conjugate Lagrange multipliers for the surprisal defined for the case of a closed algebra in the direct product space considered in Sec. IV A. The surprisal needs to be Hermitian so that, for example, the real parts of λ_1^{11} and λ_2^{11} must be equal, while the imaginary parts must have an opposite sign. At the time $t = 0$, only operators diagonal in the electronic index have non-zero Lagrange multipliers.

	$\widehat{\mathbb{I}}_N$	$\hat{a}$	$\hat{a}^\dagger$	$\hat{a}^\dagger\hat{a}$
$\|1\rangle\langle 1\|$	$\|1\rangle\widehat{\mathbb{I}}_N\langle 1\|;\lambda_0^{11}$	$\|1\rangle\hat{a}\langle 1\|;\lambda_1^{11}$	$\|1\rangle\hat{a}^\dagger\langle 1\|;\lambda_2^{11}$	$\|1\rangle\hat{a}^\dagger\hat{a}\langle 1\|;\lambda_3^{11}$
$\|2\rangle\langle 2\|$	$\|2\rangle\widehat{\mathbb{I}}_N\langle 2\|;\lambda_0^{22}$	$\|2\rangle\hat{a}\langle 2\|;\lambda_1^{22}$	$\|2\rangle\hat{a}^\dagger\langle 2\|;\lambda_2^{22}$	$\|2\rangle\hat{a}^\dagger\hat{a}\langle 2\|;\lambda_3^{22}$
$\|1\rangle\langle 2\|$	$\|1\rangle\widehat{\mathbb{I}}_N\langle 2\|;\lambda_0^{12}$	$\|1\rangle\hat{a}\langle 2\|;\lambda_1^{12}$	$\|1\rangle\hat{a}^\dagger\langle 2\|;\lambda_2^{12}$	$\|1\rangle\hat{a}^\dagger\hat{a}\langle 2\|;\lambda_3^{12}$
$\|2\rangle\langle 1\|$	$\|2\rangle\widehat{\mathbb{I}}_N\langle 1\|;\lambda_0^{21}$	$\|2\rangle\hat{a}\langle 1\|;\lambda_1^{21}$	$\|2\rangle\hat{a}^\dagger\langle 1\|;\lambda_2^{21}$	$\|2\rangle\hat{a}^\dagger\hat{a}\langle 1\|;\lambda_3^{21}$

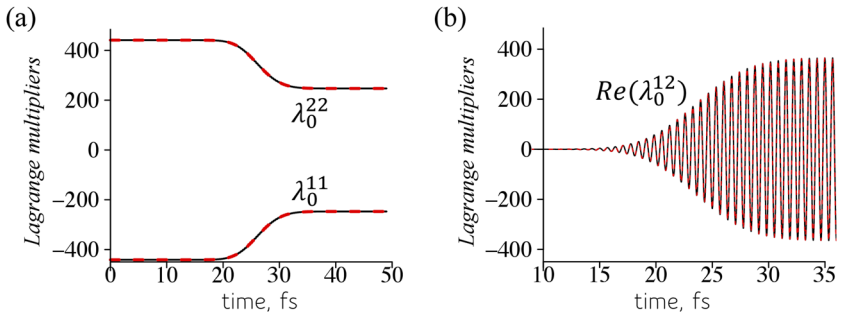

FIG. 2. Dynamics of the Lagrange multipliers for the electronic states computed from the analytical equations of motion (dashed lines) and direct propagation of the surprisal (solid lines) in a basis of vibrational states using Eq. (19). (a) Contrast the difference between the initial values of λ_0^{11} and λ_0^{22} (Lagrange multipliers of the electronic constraints $|1\rangle\langle 1|$ and $|2\rangle\langle 2|$, respectively) that serves to make the initial state essentially a pure state on the ground electronic state. As the light pulse acts and some population moves to the excited state, this difference between the Lagrange multipliers closes. (b) The multiplier for the coherence $|1\rangle\langle 2|$ between the two electronic states. Initially, the upper electronic state is empty. After the pulse, the coherence oscillates in time with a frequency that is the difference in the energy V_0 of the two states.

and results for the excitation induced by a fast laser pulse are shown in Sec. S3 2 of the supplementary material.

The algebra identified in Table I is closed for the Hamiltonian of Eq. (25) including the pulsed laser excitation. It follows that Eq. (27) for the initial state remains valid also at later times with the simple modification that the Lagrange multipliers are time-dependent. Figures 2 and 3 show time-dependent Lagrange multipliers, including the one for the coherence between the two electronic states λ_0^{12} that is zero in the initial state.

Matrix representation of the surprisal for a closed algebra. The concept of a closed algebra is nicely illustrated in terms of the matrix representation of the surprisal in a basis of the eigenstates of a harmonic oscillator (see Fig. 4). For ease of drawing, we show the matrix for a nuclear subspace only. The complete surprisal matrix is a direct product of this matrix for a nuclear subspace and a two by two matrix for the electronic subspace. In terms of this complete matrix, we are looking at one block of it.

As shown in Fig. 4, the matrix elements of the number operator $\hat{a}^\dagger\hat{a}$ are along the diagonal. The matrix elements of the $\hat{a}$ and $\hat{a}^\dagger$ are below and above the diagonal. This tridiagonal surprisal matrix is already sufficient when the algebra is closed. When the algebra is not closed, other operators may contribute based on the equations of motion for the constraints. For example, one would want to add matrix elements twice removed down and up from the diagonal. These are matrix elements of the operators $\hat{a}^{2\dagger}$ and $\hat{a}^2$. The penta-diagonal matrix as shown in Fig. 4 will be found in the open algebra case of Sec. IV B to be a reasonably accurate approximation for the surprisal. Indeed, successive iterations of the equations of motion for the Lagrange multipliers will systematically generate elements further removed from the diagonal.

2. Beyond a closed algebra

In Sec. IV A 1, a set of four operators $|1\rangle\widehat{\mathbb{I}}_N\langle 1|; |1\rangle\hat{a}\langle 1|; |1\rangle\hat{a}^\dagger\langle 1|; |1\rangle\hat{a}^\dagger\hat{a}\langle 1|$ (see Table I) were sufficient to describe the vibrational dynamics in the ground electronic state and its total population. Similarly, for the excited state plus an additional operator describing the coherence between the two electronic states, $|1\rangle\widehat{\mathbb{I}}_N\langle 2|$. We break this ideal situation by allowing the electronic transition dipole between the two electronic states to depend on the nuclear displacement. Physically, this is a common situation because the ground and more often the excited states change their electronic configuration as the bond displacement is changing. This results in a stronger correlation between the electronic and nuclear dynamics because, on a fast time scale, the motion of the nuclear wave packets modulates the strength of the electronic coupling. In a stationary picture, this results in a broad distribution of the Franck–Condon factors. An illustration of this effect for the Hamiltonian used in Sec. IV A 1,

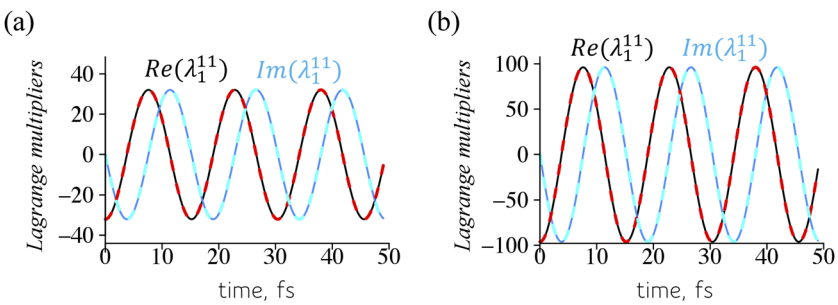

FIG. 3. Dynamics of the Lagrange multiplier for the constraint $|1\rangle\hat{a}\langle 1|$ computed from the analytical equations of motion (dashed lines) and direct propagation of the surprisal (solid lines). The initial state is displaced to a left turning point of the vibrational motion, so it has no momentum, $\langle a - a^\dagger\rangle = 0$. The initial displacement, $\boldsymbol{\delta}$, proportional to $\langle a + a^\dagger\rangle$, is (a) small and (b) large.

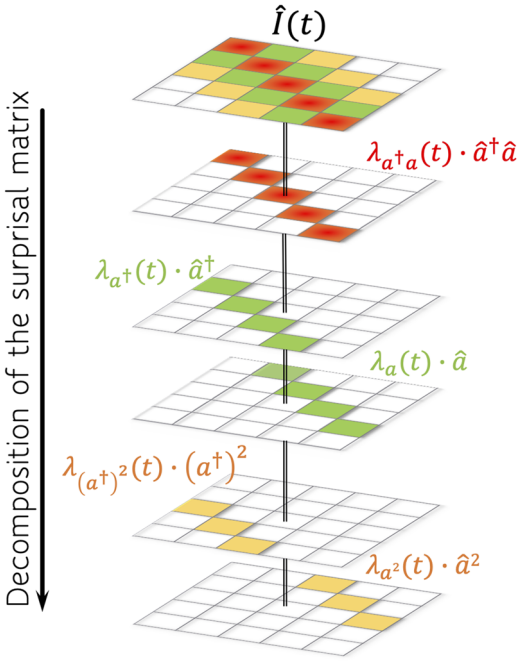

FIG. 4. Decomposition of the matrix of the surprisal $\hat{I}(t)$ for the nuclear subspace only using a zero-order vibrational basis. Results are shown for a set of time-independent constraints with time-dependent Lagrange multipliers, not including the identity operator. The algebra of the creation and annihilation operators provides a very transparent view: each operator describes a specific band in the matrix of the surprisal as highlighted with the color. The Lagrange multipliers of the Hermitian conjugates, for example, $\hat{a}$ and $\hat{a}^\dagger$, are related as $\lambda_a = (\lambda_{a^\dagger})^*$ to keep the Hermitian property of the surprisal.

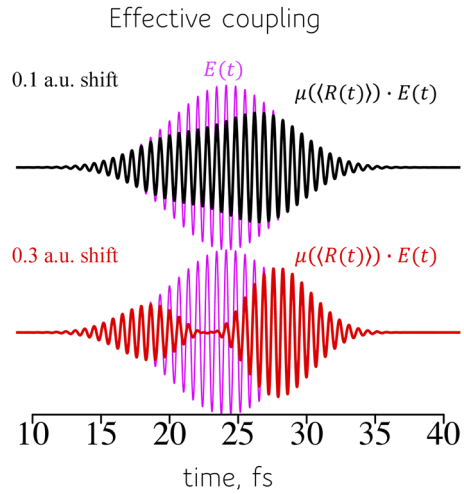

FIG. 5. Time-dependence of the effective coupling to the field due to nuclear motion of the wave packet on the ground electronic state. Shown is the field times dipole coupling term, $\hat{\mu}(\langle R\rangle(t))$, computed at the mean value $\langle R\rangle(t)$ of the time-dependent ground electronic state wave packet.

Eq. (26), is shown in Fig. 5. We use the two initial vibrational states as in Sec. IV A 1 (see Fig. S1 of the supplementary material). In one case, $\delta = 0.1$ a.u., the initial wave packet is hardly displaced from the equilibrium. In the other case, $\delta = 0.3$ a.u., the initial wave packet is quite displaced from equilibrium such that the most probable initial vibrational state is $v = 5$.

The dipole is defined to be a linear function of the nuclear coordinate, $\hat{\boldsymbol{\mu}}(R) = \boldsymbol{\mu_0} + \boldsymbol{\mu_1}\cdot(\hat{a}+\hat{a}^\dagger)$, with the specific choice $\boldsymbol{\mu_0} = 0.8$ and $\mu_1 = 0.175$. The small initial shift of the ground state wave packet of 0.1 a.u. [see Fig. S1(a) of the supplementary material] induces the oscillation of the mean value $\langle R\rangle$ in the range from −0.1 to 0.1; therefore, the dipole varies from 0.52 to 1.08. The larger initial shift, 0.3 a.u. [see Fig. S1(b) of the supplementary material], results in the dipole oscillation from −0.04 to 1.6, giving rise to an effectively dark state at the time when the field is at its maximum (red curve in Fig. 5).

Equations of motion when the algebra is not closed. Section S3 1 of the supplementary material discusses the systematic results for the equations of motion for the initial set of constraints for the Hamiltonian we use in Sec. IV, Eq. (25), when the transition dipole moment depends linearly on the bond displacement R, $\hat{\boldsymbol{\mu}} = \boldsymbol{\mu_0} + \boldsymbol{\mu_1}\cdot(\hat{a}+\hat{a}^\dagger)$, where we express the bond displacement in terms of creation and annihilation operators in the algebra. When $\mu_1 = 0$, the algebra is closed. When $\mu_1 \neq 0$, the closure is broken in a very systematic way. The full details are in Sec. S3 1 of the supplementary material. Here, we exhibit the rate of change of the population in, say, the ground electronic state. The explicit result is

$$-\frac{i}{\hbar}\left[\hat{H}, |1\rangle\widehat{\mathbb{I}}_N\langle 1|\right] = -\frac{i}{\hbar}\boldsymbol{\mu_0}E(t)\left(|1\rangle\widehat{\mathbb{I}}_N\langle 2| - |2\rangle\widehat{\mathbb{I}}_N\langle 1|\right) - \frac{i}{\hbar}\boldsymbol{\mu_1}E(t)\left(|1\rangle(\hat{a}+\hat{a}^\dagger)\langle 2| - |2\rangle(\hat{a}+\hat{a}^\dagger)\langle 1|\right). \tag{28}$$

When $\mu_1 = 0$, the dynamics of the electronic constraint, $|1\rangle\widehat{\mathbb{I}}_N\langle 1|$, is coupled only to the electronic constraints, $|1\rangle\widehat{\mathbb{I}}_N\langle 2|$ and $|2\rangle\widehat{\mathbb{I}}_N\langle 1|$. The population rate of change is determined only by the electronic coherences. When $\mu_1 = 0$, the four electronic basis states $|1\rangle\langle 1|$, $|2\rangle\langle 2|$, $|1\rangle\langle 2|$, and $|2\rangle\langle 1|$ form a closed electronic sub-algebra, but this is broken when $\mu_1 \neq 0$. The same structure is maintained for, say, the rate of change of the displacement of the wave packet on the ground electronic state, $-i\left[\hat{H}, |1\rangle(\hat{a}+\hat{a}^\dagger)\langle 1|\right]$,

$$\begin{aligned}-\frac{i}{\hbar}\left[\hat{H}, |1\rangle(\hat{a}+\hat{a}^\dagger)\langle 1|\right] &= i\boldsymbol{\omega}|1\rangle(\hat{a}-\hat{a}^\dagger)\langle 1| - \frac{i}{\hbar}\boldsymbol{\mu}_0E(t)\left(|1\rangle(\hat{a}+\hat{a}^\dagger)\langle 2| - |2\rangle(\hat{a}+\hat{a}^\dagger)\langle 1|\right)\\ &- \frac{i}{\hbar}\boldsymbol{\mu_1}E(t)\left(|1\rangle\widehat{\mathbb{I}}_N\langle 2| - |2\rangle\widehat{\mathbb{I}}_N\langle 1|\right)\\ &- \frac{i}{\hbar}2\boldsymbol{\mu_1}E(t)\left(|1\rangle\hat{a}^\dagger\hat{a}\langle 2| - |2\rangle\hat{a}^\dagger\hat{a}\langle 1|\right)\\ &- \frac{i}{\hbar}\boldsymbol{\mu_1}E(t)\left(|1\rangle\left(\hat{a}^2+(\hat{a}^\dagger)^2\right)\langle 2| - |2\rangle\left(\hat{a}^2+(\hat{a}^\dagger)^2\right)\langle 1|\right).\end{aligned} \tag{29}$$

In Eq. (28), we see that when $\mu_1 \neq 0$, the electronic constraint is affected by the nuclear constraints, for example, $|1\rangle\hat{a}\langle 2|$. In turn, the rate of change of the mean position, Eq. (29), will have contribution of the operators that are quadratic in the creation or annihilation operators. This is already not in the algebra $\{\hat{\mathbb{I}}_N, \hat{a}, \hat{a}^\dagger, \hat{a}^\dagger\hat{a}\}$. The rate of change in the vibrational energy in the ground electronic state $-i[\hat{H}, |1\rangle(\hat{a}^\dagger\hat{a})\langle 1|]$ when $\mu_1 \neq 0$ has terms of operators that are cubic in the creation or annihilation operators and so on.

The matrix representation of the surprisal when the algebra is not closed. We consider the surprisal as a matrix in a basis of vibrational states. Let us compare to the case when the algebra is closed as in Sec. IV A. In this basis, the matrix elements of $\hat{a}^\dagger\hat{a}$ are along the diagonal. The matrix elements of $\hat{a}^\dagger$ and $\hat{a}$ are above and below the diagonal. Hence, for the cases discussed in Sec. IV A 1, the exact surprisal matrix is strictly tridiagonal. Now, in this section, the algebra is not closed. One could expect, however, that a tridiagonal matrix can be a good approximation, and we show below that this is indeed the case for the initial state that is shifted on a small extent. To stay at the same level of accuracy for the initial state that is larger shifted, we need to add more constraints. These correspond to matrix elements of $\hat{a}^{\dagger 2}$ and $\hat{a}^2$ of the nuclear sub-space leading to a penta-diagonal matrix, as shown in Fig. 4. This will turn out to be an acceptable approximation for both initial states. A general way to describe the contribution of each of the operators is by computing their Lagrange multipliers via Eq. (24). Strictly speaking, one can go on symmetrically adding terms further above and below the diagonal just so that the matrix will remain Hermitian. The error when keeping terms up to the fourth power in $\hat{a}^\dagger$ or $\hat{a}$ is shown in Fig. S4 of the supplementary material. As is clear, this ennea-diagonal surprisal matrix is about as off-diagonal as is warranted to extend toward an acceptably small, say, below 1 pml, numerical error.

Electronic dynamics. Figure 6 shows the electronic population and coherence for the two dipoles shown in Fig. 5. This is a case for which the algebra is not closed. The approximate computation of the surprisal keeps off diagonal terms in the oscillator basis up to the fourth rank off the diagonal. Note that this level is sufficient to reproduce the time evolution of the electronic populations in the case of the highly shifted initial state up to a high level of numerical accuracy. As shown in Fig. 5, for this case at early times of the interaction with a pulse, around 20 fs–25 fs, the transition is almost dark, and it takes some time for the wave packet to move out of the region in the displacement where the dipole is small. This is reflected in both exact and approximate treatments of the surprisal [see Figs. 6(c) and 6(d)].

The nine observables that are kept in the surprisal computation in Fig. 6 suffice equally to reproduce even the fine details of the vibrational state distribution, as shown in Fig. S5 of the supplementary material. The highly vibrationally displaced initial state and the resulting almost dark transition (see Fig. 5) are a severe test for an approximate surprisal. Figure 6 shows that one can obtain quite acceptable accuracy by keeping enough terms. Figure 7 shows that there is an even smaller but a dominant set of constraints. For the initial state with only few vibrational states in the superposition, this is the set $\{\hat{\mathbb{I}}_N, \hat{a}, \hat{a}^\dagger, \hat{a}^\dagger\hat{a}\}$, the set that is the closed algebra when the dipole is not R-dependent. It corresponds to a tridiagonal surprisal matrix. This set is sufficient for the vibrational distribution on the excited electronic state [see, e.g., Fig. 7(b)], but not fully during the pulse, for the ground state [Fig. 7(a)]. For the highly vibrationally excited initial state [see Figs. 7(c) and 7(d)], it is necessary to use a

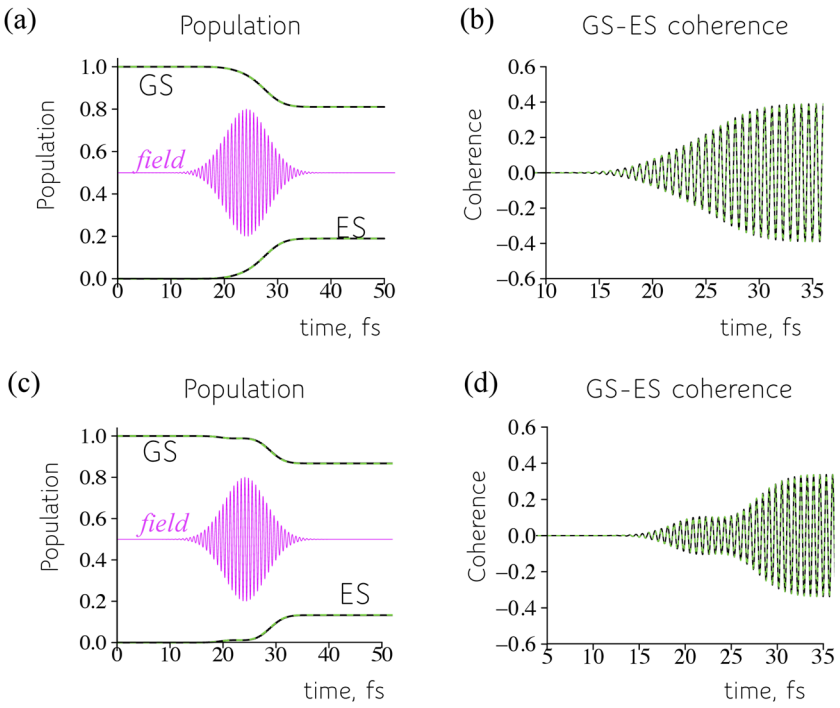

FIG. 6. Electron dynamics for an initial state that is [(a) and (b)] only slightly displaced from vibrational equilibrium, $\langle R(0)\rangle$ = 0.1 a.u. and [(c) and (d)] displaced on a larger extent [$\langle R(0)\rangle$ = 0.3 a.u.]. [(a) and (c)] Dynamics of the population in the ground (GS) and excited (ES) electronic states and [(b) and (d)] time-evolution of the coherence between the two electronic states. Comparison of the mean values calculated from the surprisal propagated on a finite basis of 20 vibrational states (black solid lines) vs an ennea-diagonal surprisal matrix reconstructed from the Lagrange multipliers for the set of constraints: $\{\hat{\mathbb{I}}_N, \hat{a}^k, (\hat{a}^\dagger)^k, \hat{a}^\dagger\hat{a}\}$, $k = 1, \ldots, 4$. The algebra is not closed, and the error in the approximate computation, below 1 pml after the initial times, is finite but small as shown in Fig. S4 of the supplementary material. The profile of the field is shown as a pink trace.

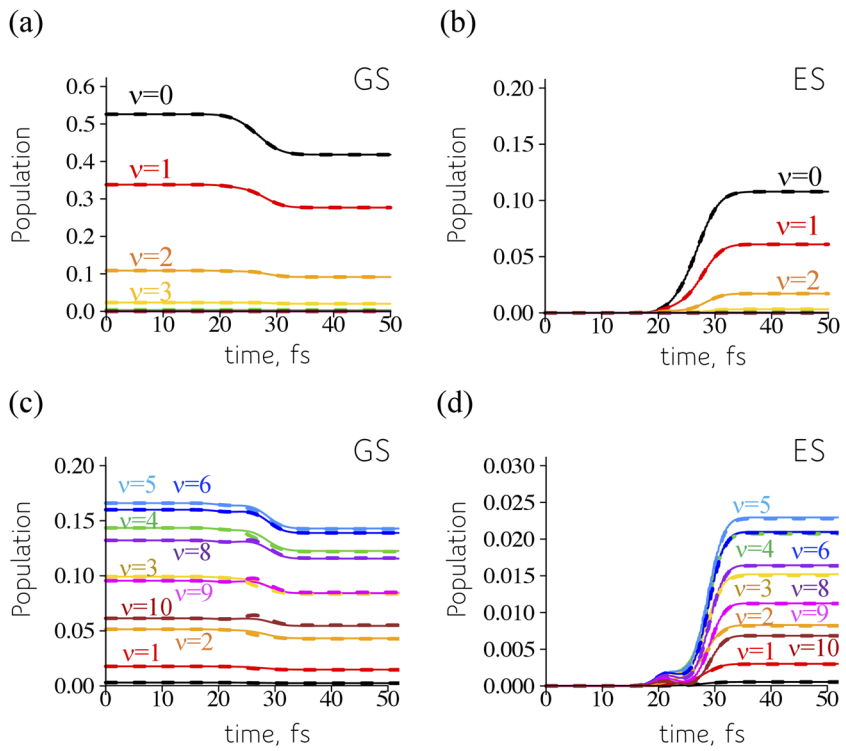

FIG. 7. Population of the different vibrational states in the ground [(a) and (c)] and excited [(b and (d)] electronic states computed from the approximate surprisal (dashed lines) and from exact surprisal (solid lines). Shown are the results [(a) and (b)] for the small displacement of the initial state and using only the dominant constraints $\left\{\widehat{\mathbb{I}}_N, \hat{a}, \hat{a}^\dagger, \hat{a}^\dagger\hat{a}\right\}$ in the approximate surprisal and [(c) and (d)] for the large shift of the initial state using the six constraints $\left\{\widehat{\mathbb{I}}_N, \hat{a}, \hat{a}^\dagger, \hat{a}^\dagger\hat{a}, \hat{a}^2, (\hat{a}^\dagger)^2\right\}$.

larger set of a penta-diagonal surprisal, $\left\{\widehat{\mathbb{I}}_N, \hat{a}, \hat{a}^\dagger, \hat{a}^2, (\hat{a}^\dagger)^2, \hat{a}^\dagger\hat{a}\right\}$, a set of dominant constraints.

The Lagrange multipliers. Even when the algebra is not closed, one can determine the value of the Lagrange multiplier that is conjugate to a given operator. This corresponds to seeking a density matrix of maximal entropy subject to a given expectation value of this operator. An accurate representation of the density will often require imposing the mean values of several constraints, as shown, for example, in Fig. 7. Defining the numerical value of the Lagrange multiplier by the condition that the density reproduces the mean value of the conjugate observable leads to an implicit, transcendental, equation. Solving this equation is not fully trivial even in the classical limit when the observables commute.[37] When the observables do not commute handling, an exponent that is a linear sum of observables adds at least one additional layer of complexity. The advantage of proceeding via the surprisal route is that it deals with the linear sum rather than with the exponent thereof. A Lagrange multiplier can thereby be determined directly from the surprisal, as discussed in Sec. III B. A simple summary of the key result, Eq. (24), is to take the Hilbert–Schmidt scalar product of the operator of interest with the surprisal.

Under ordinary circumstances, one thinks of the Lagrange multiplier conjugate to the number operator, $\hat{N} = \hat{a}^\dagger\hat{a}$, as the temperature. The multiplier for the oscillator in the case of an open algebra is shown in Fig. 8. When the transition dipole does not depend on the nuclear displacement, the Franck–Condon factors allow only vertical transitions; therefore, the Lagrange multipliers for $|1\rangle\hat{N}\langle 1|$ and $|2\rangle\hat{N}\langle 2|$ operators are constant, and there is no contribution of the off-diagonal constraint $|1\rangle\hat{N}\langle 2|$ to the density. In this subsection, when the dipole is changing with the displacement, the situation, as shown, is more complex.

The Lagrange multipliers are conjugate to the observables. This means that, in principle, they can be used to describe the state of the system in a manner complementary to that of the expectation values of the observables. A clear example is provided in Fig. 8(a). At the peak of the short pulse, there is significant depletion of the ground state, but as the pulse weakens, some states that were electronically excited during the pulse revert back to the ground electronic state. The vibrational temperature in the excited state goes down to a finite lower value. Eventually, the pulse does induce a net population transfer, but not as much as during the pulse. The Lagrange multipliers for the electronic energy transfer are shown in Fig. S6 of the supplementary material. As is evident, it is not very different from Fig. 4 that shows these multipliers for the case of a closed algebra.

Not only the electronic coherence but also the coherence between different vibrational states on the same electronic state is well reproduced. Figure 9 shows results both for the vibrations on the excited electronic state, states that are not populated before the pulse and for the vibrations on the ground electronic state. The solid lines are computations of a numerically exact surprisal using a basis of 20 vibrational states on each electronic state. The two panels on the left are for an initial vibrational state that is not very displaced. For this case, the smallest set of operators for the vibrations, $\left\{\widehat{\mathbb{I}}_N, \hat{a}, \hat{a}^\dagger, \hat{a}^\dagger\hat{a}\right\}$, is sufficient for an acceptable accuracy [see dashed lines in Fig. 9(a)]. This is consistent with our earlier

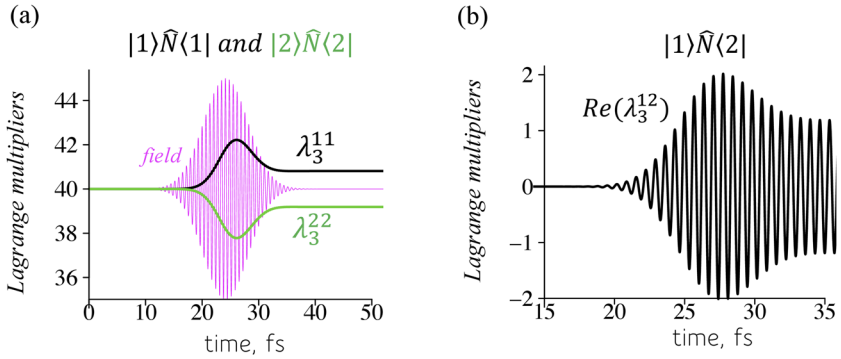

FIG. 8. Lagrange multipliers for the number operator $\hat{N} = \hat{a}^\dagger\hat{a}$. (a) The operators diagonal in the electronic state index have real-valued Lagrange multipliers. The superscripts on the Lagrange multipliers designate the two electronic states, and the subscript is an index of the operator (see Table I and Sec. S3 1 of the supplementary material). In contrast to the closed algebra case, the Lagrange multiplier of the number operator is changing in time, and in an opposite way for the ground and excited electronic states (black and green line, respectively). (b) The off-diagonal in the electronic state index number operator has a much smaller Lagrange multiplier that beats with the frequency of the energy gap between the two electronic states. As the two potentials are the same, the gap does not depend on the nuclear coordinate; therefore, there is only a constant beating frequency. These Lagrange multipliers are the same for the two initial states (with small and large displacement of the initial state) considered.

results for the closed algebra. When the initial state is more displaced so that higher vibrational states are accessed, we need a bigger set, $\left\{\widehat{\mathbb{I}}_N, \hat{a}, \hat{a}^\dagger, \hat{a}^2, (\hat{a}^\dagger)^2\hat{a}^\dagger\hat{a}\right\}$ [see dashed lines in Fig. 9(b)]. The coherence oscillates with the frequency difference between the two vibrational states. When the initial state is more displaced, we show the coherence between states with a larger difference in their vibrational quantum numbers to emphasize the accuracy of the approximation.

Counteracting the migration of matrix elements of the surprisal away from the diagonal is the decline in the value of the conjugate Lagrange multipliers. Figure 10 shows the computed multipliers for three successive powers, $\hat{a}, \hat{a}^2$, and $\hat{a}^3$. The successive values decline by two orders of magnitude per increasing power. To a limited extent, this is compensated by the successive mean value being somewhat higher, but the overall tendency is that the terms that originate in the failure of the algebra to close do not contribute significantly. The dominant constraints in the surprisal are the trio $\hat{a}, \hat{a}^\dagger$, and $\hat{a}^\dagger\hat{a}$ that generate the tridiagonal structure of the surprisal matrix. This set of constraints is sufficient when the algebra is closed. Adding $\hat{a}^2$ and $(\hat{a}^\dagger)^2$ as constraints leads to a

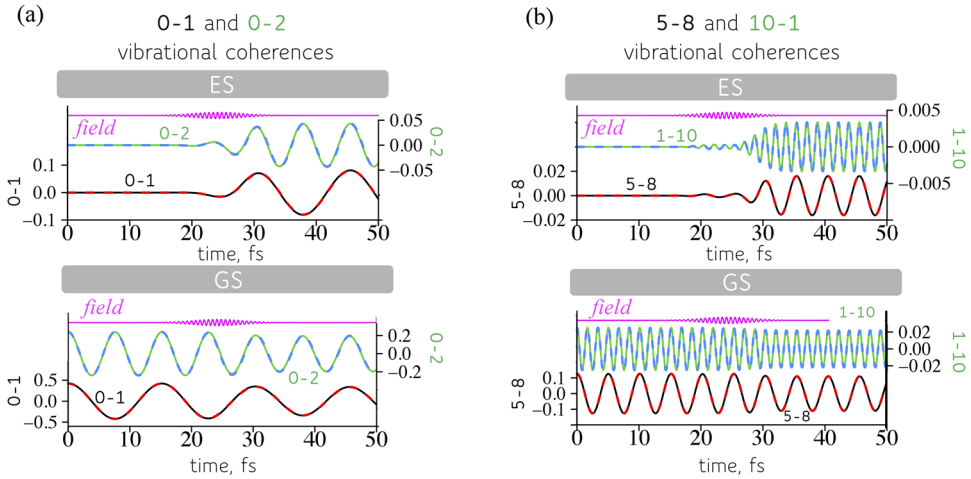

FIG. 9. Exact coherence of vibrational states (solid lines) and their approximation (dashed lines) using a dominant set of constraints for the small (a) and large (b) shift of the initial state. (a) Coherence of the ground vibrational state $v = 0$ and neighboring $v = 1$ state (black and red lines) and $v = 0$ and $v = 2$ states (green and blue lines) for the ground (GS, bottom panel) and excited (ES, top panel) electronic states. The smallest possible set of operators is accurate, a set that is closed if the dipole is constant, which is not the case here. (b) An initial state that is peaked at the fifth vibrational state (see Fig. S1 of the supplementary material), and higher vibrational states can be accessed (see Fig. 7). Shown are the coherences of the neighboring $v = 5$ and $v = 8$ states (black and red lines), and $v = 1$ and $v = 10$ states (green and blue lines). A bigger set of nuclear constraints, $\left\{\widehat{\mathbb{I}}_N, \hat{a}, \hat{a}^\dagger, \hat{a}^2, (\hat{a}^\dagger)^2\hat{a}^\dagger\hat{a}\right\}$, is needed for a fully realistic approximation.

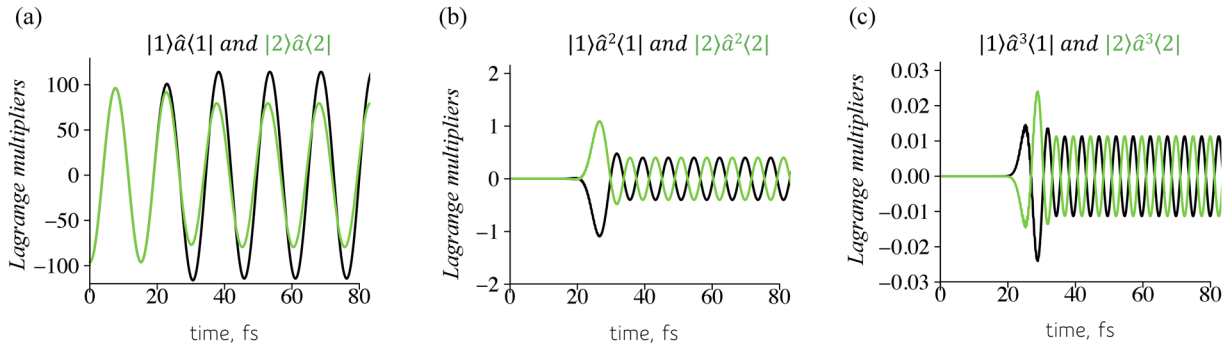

FIG. 10. Lagrange multipliers for three successive powers of the creation operator as indicated on the plots: (a) first power, (b) second power, and (c) third power. Black curves correspond to the ground electronic state operators and green curves to the excited state operators. Shown are the results of the surprisal computation for the large shift of the initial state.

penta-diagonal surprisal and, as discussed above, is a sufficiently accurate approximation.

As dynamics unfolds on several electronic states and the coherence effects are prominent [the rate of change of the populations is determined by the coherences, see Eq. (S3.8) of the supplementary material], it needs several dominant constraints in each electronic state. However, it is still much less, as compared to the universal finite basis representation (or the Gelfand basis, $\mathbf{E}_{nm}$) (see Table II). The benefit is already seen for the small basis of vibrational states, 400 vs 16 constraints in the Gelfand and $\{\widehat{\mathbb{I}}_N, \hat{a}, \hat{a}^\dagger, \hat{a}^\dagger\hat{a}\} \otimes \{\widehat{\mathbb{I}}_e, \hat{\boldsymbol{\sigma}}_x, \hat{\boldsymbol{\sigma}}_y, \hat{\boldsymbol{\sigma}}_z\}$ representation, respectively. Increasing the number of vibrational basis functions needed for an accurate representation of the initial state requires 24 dominant constraints out of 1600 in the more universal Gelfand representation.

The entries under dominant constraints in Table II assume that all the four electronic constraints are important. As we discuss in Sec. IV B, this need not be the case. For example, in the smallest dominant case, already the set $\{\widehat{\mathbb{I}}_N, \hat{a}^\dagger\hat{a}\} \otimes \{\widehat{\mathbb{I}}_e, \hat{\boldsymbol{\sigma}}_z\} + \{\hat{a}, \hat{a}^\dagger\} \otimes \{\widehat{\mathbb{I}}_e, \hat{\boldsymbol{\sigma}}_x, \hat{\boldsymbol{\sigma}}_y, \hat{\boldsymbol{\sigma}}_z\}$ is essential for a fully realistic description. This cuts it down from 16 to 12 operators, but it is not a significant reduction compared to the reduction from the 400 that one needs to keep in the fully accurate Gelfand representation.

B. A toy model for an internal conversion in pyrazine

In Sec. IV A, we discussed the dynamics when two electronic states are coupled by a fast transient pulse. Here, we describe the dynamics when two electronic states are coupled by diabatic coupling that is acting throughout. Our model is a toy version of the model of two electronic states and three vibrational modes used by Schneider and Domcke[36,38] to simulate internal conversion in pyrazine. We use only the $\boldsymbol{\nu}_{10a}$ coupling mode that couples the two diabatic electronic states with a coupling that is a linear function of nuclear distance, $\hat{V} = \kappa(\hat{a} + \hat{a}^\dagger)$. From the algebraic point of view it is the analog of the dipole moment that linearly depends on the displacement of Sec. IV A, but, here, the coupling is acting throughout. In either case, the algebra is not closed and for the same reason. The parameters of the two potentials are shown in Table S6 of the supplementary material. There is a low barrier at the equilibrium position in the adiabatic picture, and this will be reflected in the shape of the wave packet as it moves on the ground state potential.

1. Non-adiabatic dynamics

We initiate the dynamics on the excited electronic state with an initial vibrational state slightly shifted to the right of the equilibrium

TABLE II. The number of the constraints needed to represent the surprisal and the density matrix. The finite basis representation, the Gelfand basis, is universal but not compact. Also shown are the dominant constraints that describe almost the same amount of information but with a fewer number of operators.

	Gelfand basis	Dominant constraints
Small initial shift, 10 vibrational basis functions per electronic state	$10 \times 10 \times 4 = 400$	$4 \times 4 = 16$ $\{\widehat{\mathbb{I}}_N, \hat{a}, \hat{a}^\dagger, \hat{a}^\dagger\hat{a}\} \otimes \{\widehat{\mathbb{I}}_e, \hat{\boldsymbol{\sigma}}_x, \hat{\boldsymbol{\sigma}}_y, \hat{\boldsymbol{\sigma}}_z\}$
Large initial shift, 20 vibrational basis functions per electronic state	$20 \times 20 \times 4 = 1600$	$6 \times 4 = 24$ $\{\widehat{\mathbb{I}}_N, \hat{a}, \hat{a}^\dagger, \hat{a}^2, (\hat{a}^\dagger)^2\hat{a}^\dagger\hat{a}\} \otimes \{\widehat{\mathbb{I}}_e, \hat{\boldsymbol{\sigma}}_x, \hat{\boldsymbol{\sigma}}_y, \hat{\boldsymbol{\sigma}}_z\}$

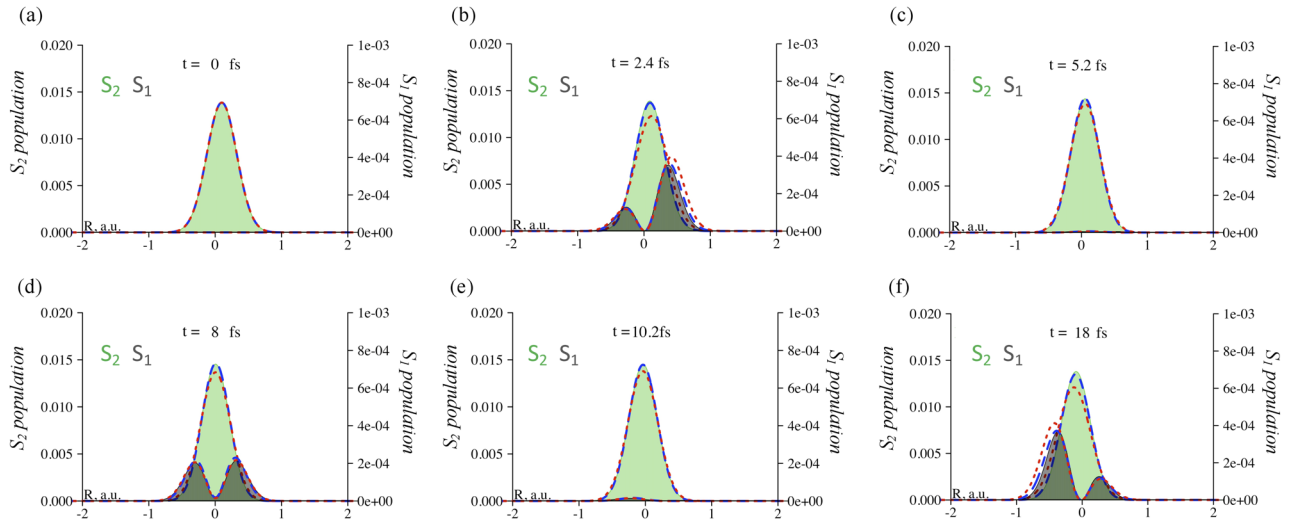

FIG. 11. Population exchange between the two electronic states due to diabatic coupling, $\hat{V} = \kappa(\hat{a} + \hat{a}^\dagger)$. Computed by the time propagation of the surprisal on a finite vibrational basis. The wave packet density on the upper electronic state is plotted in light green and in dark gray on the lower electronic state. Panels (a)–(f) are computed for increasing time values as indicated. Also shown are two approximate computations where the surprisal is expanded in a minimal basis of dominant constraints $\{\widehat{\mathbb{I}}_N, \hat{a}, \hat{a}^\dagger, \hat{a}^\dagger\hat{a}\}$ (red dotted curve) and in the extended set $\{\widehat{\mathbb{I}}_N, \hat{a}, \hat{a}^\dagger, \hat{a}^2, (\hat{a}^\dagger)^2\hat{a}^\dagger\hat{a}\}$ for the nuclear constraints (blue dashed curve).

point. The surprisal is propagated on a basis of 20 vibrational functions per electronic state, and in addition, we compute two approximations where the surprisal is expanded using only a dominant set of constraints. The approximate computations use a minimal and a slightly larger basis of operators as identified in Table II. We process the time-dependent surprisal to determine the population in each electronic state as a function of time and nuclear coordinate (see Fig. 11). The diabatic coupling induces rather fast exchange of the population between the two states. Even just the minimal set of three vibrational constraints, dashed red curve, provides a fully realistic approximation that deviates only when the wave packet is near its outer turning point on the ground state. It is worthwhile to point out that the minimal set of dominant constraints means that the four blocks of the surprisal matrix (each one for the different electronic constraints) when written in the finite basis are tridiagonal. It is as minimally coherent as can be, yet it offers a fully realistic view of the dynamics. The larger basis of constraints, blue dashed curve, is exact to graph reading accuracy. This somewhat larger basis, Table II, consists of adding just two vibrational constraints, $\hat{a}^2$ and $(\hat{a}^\dagger)^2$, to the minimal basis.

The considerable insight offered by the dominant constraints is also seen in the computed population and coherences integrated over the nuclear coordinate (see Fig. 12). Already the minimal basis set of constraints, while somewhat deviant near the turning points (see Fig. 11), captures such subtle features as the oscillation of the electronic coherence due to the slow vibrational motion, a period of 35 fs [see Fig. 12(b)]. The out of phase motion of the population of the excited state and the coherence is to be expected because the maximal coherence is when the population of the excited state is maximally depleted.

2. A minimal set for the electronic degrees of freedom

Throughout, we have taken note that many operators on the vibrational states, e.g., $(a^\dagger a)^2$, do not have a significant weight as

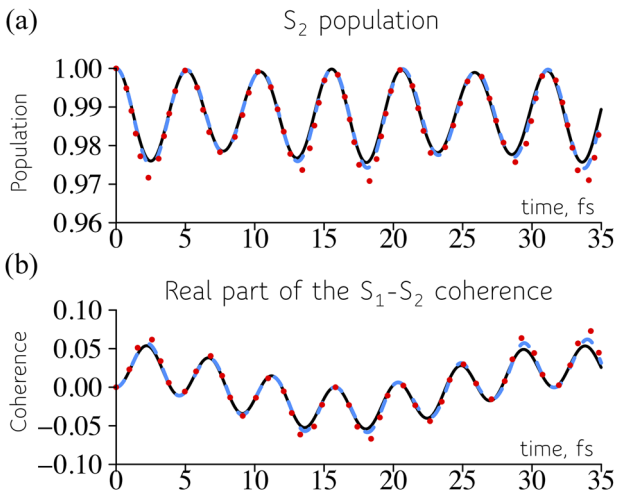

FIG. 12. Population of the upper electronic state (a) and the electronic coherence (b). Solid black curve: numerically accurate computations of the time-dependent surprisal propagated on a finite vibrational basis. Red dots: a minimal set of dominant constraints is used to expand the surprisal. Blue dashed curve: the slightly augmented minimal set of constraints is used. The fast oscillations are due to the electronic energy difference of about 7260 cm^{-1} or almost eight times faster than a vibrational period.

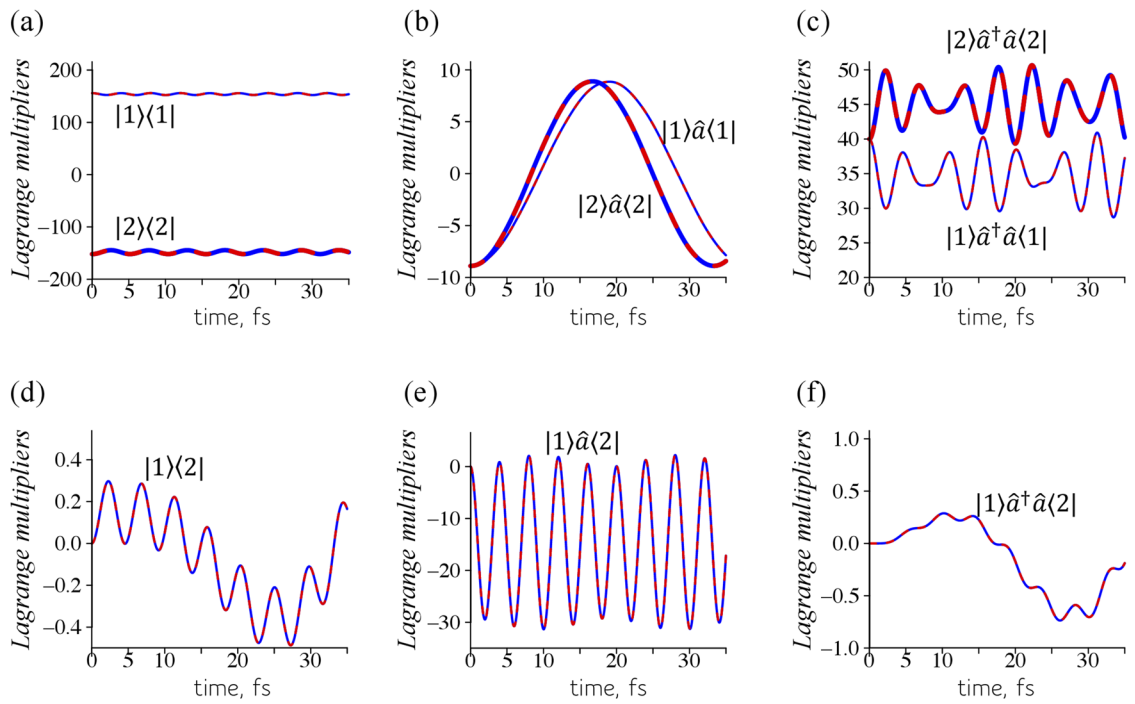

FIG. 13. Lagrange multipliers for a radiationless transition for constraints: diagonal [(a)–(c)] and off-diagonal [(d)–(f)] in the electronic index. Shown are the results for the two dominant bases discussed in Table II. Both have the same electronic part, $\{\widehat{\mathbb{I}}_e, \hat{\boldsymbol{\sigma}}_x, \hat{\boldsymbol{\sigma}}_y, \hat{\boldsymbol{\sigma}}_z\}$. The blue curve for the slightly larger vibrational set is already quite accurate (see, for example, Fig. 12). The red dashed curve is the minimal vibrational set. The two curves agree as a direct consequence of the orthogonality of the constraints—extension to a larger number of constraints does not affect the Lagrange multipliers of the initial set. Comparing panels (a) and (d), one sees that the electronic multiplier for the operator $|1\rangle\langle 2|$ can be neglected. Similarly, by comparing panels (c) and (f), the electronic multiplier for the operator $|1\rangle a^\dagger a\langle 2|$ can almost be neglected. Yet, comparing panels (b) and (e), $|1\rangle\hat{a}\langle 2|$ can definitely not be neglected.

measured by their conjugate Lagrange multiplier (or, strictly speaking by their contribution to lowering the entropy, meaning that their conjugate Lagrange multiplier times their expectation value). The same is actually the case also for the operators in electronic subspace. In the minimal set $\{\widehat{\mathbb{I}}_e, \hat{\boldsymbol{\sigma}}_x, \hat{\boldsymbol{\sigma}}_y, \hat{\boldsymbol{\sigma}}_z\}$, we find that for our toy model, the operators $|1\rangle\langle 2|$ and $|2\rangle\langle 1|$ have Lagrange multipliers that can be neglected, as shown in Fig. 13.

This is unlike the operators $|1\rangle a\langle 2|$ and $|2\rangle a^\dagger\langle 1|$ that are quite dominant. The difference is due to that the electronic transition is accompanied by a gain or loss of one vibrational quantum as can be seen from the oscillation frequency of the Lagrange multiplier for the $|1\rangle a\langle 2|$ constraint, $\bar{\omega} = V_0 + \hbar\omega$. It is higher from the electronic gap V_0 by one quantum of vibration and corresponds to the period of 4 fs. Consistent with this selectivity, the Lagrange multipliers for the pair $|1\rangle a^\dagger a\langle 2|$ and $|2\rangle a^\dagger a\langle 1|$ are again negligible. The vibrational selectivity is rather likely a reflection of the linearity in the nuclear displacement of the coupling between the two electronic states. Indeed, the mean values for the population and coherence for this even smaller set of constraints are as accurate as the $\{\widehat{\mathbb{I}}_N, \hat{a}, \hat{a}^\dagger, \hat{a}^\dagger\hat{a}\} \otimes \{\widehat{\mathbb{I}}_e, \hat{\boldsymbol{\sigma}}_x, \hat{\boldsymbol{\sigma}}_y, \hat{\boldsymbol{\sigma}}_z\}$ minimal set representation (see Fig. S7 of the supplementary material).

V. CONCLUDING REMARKS

Surprisal analysis of experimental distributions in physics, chemistry, and biology can often be characterized even by a single dominant constraint. A very recent example is the analysis of COVID19 patient gene expression samples to identify a single constraint, a gene module that strongly aligns with disease severity.[39] In the present work, we go back to the foundations of the quantum mechanical methodology of the surprisal analysis. We discuss two examples of the dynamics that unfold on two electronic states. We therefore deal with the state of the system, the density matrix, on the basis of individual quantum (electronic and vibrational) states. In the absence of constraints, this density will be uniform. The presentation begins by proceeding from a Hamiltonian to a numerically exact representation of the quantum mechanical surprisal. We explain that under special circumstances (a closed algebra), the surprisal can be explicitly represented as a sum over known constraints at all times of the dynamics. The key practical points are that we outline the numerically exact route from the given initial conditions and a Hamiltonian to the quantal surprisal, a route that is always possible when we work, as we almost always do, in a finite dimensional Hilbert space. This is a predictive route from a Hamiltonian to

a surprisal, a surprisal that accurately accounts for both the populations and the coherences of the quantum states.

Another key result is a practical quantum mechanical surprisal analysis: Given an operator that is a candidate for a constraint on the dynamics and the exact surprisal, the formalism we present determines the value of its conjugate Lagrange multiplier. This is the analog of what is done by a classical surprisal plot. The added new feature is that we compute the time dependence of this multiplier during the dynamics and not only for the long time. By direct dynamical propagation of the surprisal, we obtain the matrix of the surprisal at different times of the dynamics. We evaluate the Lagrange multipliers, the coefficients of the chosen set of constraints, using the orthogonality relations established for this set of operators. We discuss both the cases when the algebra is closed, the finite set of constraints gives an exact expression of the density, and when the algebra of the constraints is not closed, the finite set of constraints provides only an approximation to the density. Our results confirm that, in the latter case, a finite set of constraints can have coefficients orders of magnitude higher than the other constraints. Among these, dominant constraints appear also operators off-diagonal in the electronic index, such as $|1\rangle\hat{a}\langle 2|$. The density build-up using only few such dominant constraints is here shown to be accurate enough to describe the effects of the vibrational and electronic coherences and the shape of the nuclear wave packets on two electronic states.

SUPPLEMENTARY MATERIAL

The supplementary material contains details regarding various technical aspects of the computation of the surprisal on a finite basis and its analysis. We focus on the time evolution of the surprisal in a direct product Hilbert space of electronic and vibrational degrees of freedom of a molecule. The well-known basis of harmonic oscillator states and the algebra of the creation/annihilation operators are used throughout. In general, a similar method can be applied to any finite basis suitable for the description of the problem of interest. In Sec. S1, we discuss the orthogonalization procedure that is used to generate a specific set of operators in a finite basis. Thereby, a unique set of Lagrange multipliers can be determined from the matrix of the surprisal computed in this finite basis. The details of the computation of the surprisal matrix are specified. Then, the computational details are given for the three cases of the dynamics as discussed in Sec. IV. In Sec. S3, the equations of motion for the constraints are given as well as the analytical equations of motion for the Lagrange multipliers that are rigorous only in the case of a closed algebra.

ACKNOWLEDGMENTS

This work was supported by the EC Horizon2020 FETOpen COPAC Project No. 766563. F.R. acknowledges support from the Fonds National de la Recherche Scientifique, Belgium (F.R.S-FNRS; Grant Nos. PDR T.0205.20 and J.0012.18).

DATA AVAILABILITY

The data that support the findings of this study are available within the article and its supplementary material.

REFERENCES

[1] M. Cho, *Two-Dimensional Optical Spectroscopy* (CRC Press, Boca Raton, 2009).
[2] S. Mukamel, *Principle of Nonlinear Optical Spectroscopy* (Oxford University Press, Oxford, 1995).
[3] E. T. Jaynes, "Information theory and statistical mechanics," Phys. Rev. **106**, 620 (1957).
[4] A. Katz, *Principles of Statistical Mechanics: The Information Theory Approach* (Freeman, San Francisco, 1967).
[5] D. N. Zubarev, *Nonequilibrium Statistical Mechanics* (Consultants Bureau, London, 1974).
[6] C. Shannon, "A mathematical theory of communication," Bell Syst. Tech. J. **27**, 379 (1948).
[7] E. H. Wichmann, "Density matrices arising from incomplete measurements," J. Math. Phys. **4**, 884–896 (1963).
[8] B. Schumacher, "Quantum coding," Phys. Rev. A **51**, 2738 (1995).
[9] S. Dagan and Y. Dothan, "Evaluation of an incompletely measured spin density matrix," Phys. Rev. D **26**, 248 (1982).
[10] Y. Alhassid and R. D. Levine, "Collision experiments with partial resolution of final states: Maximum entropy procedure and surprisal analysis," Phys. Rev. C **20**, 1775 (1979).
[11] R. D. Levine, "Information theory approach to molecular reaction dynamics," Annu. Rev. Phys. Chem. **29**, 59 (1978).
[12] F. Remacle, N. Kravchenko-Balasha, A. Levitzki, and R. D. Levine, "Information-theoretic analysis of phenotype changes in early stages of carcinogenesis," Proc. Natl. Acad. Sci. U. S. A. **107**, 10324 (2010).
[13] S. Zadran, R. Arumugam, H. Herschman, M. E. Phelps, and R. D. Levine, "Surprisal analysis characterizes the free energy time course of cancer cells undergoing epithelial-to-mesenchymal transition," Proc. Natl. Acad. Sci. U. S. A. **111**, 13235 (2014).
[14] N. Kravchenko-Balasha, J. Wang, F. Remacle, R. D. Levine, and J. R. Heath, "Glioblastoma cellular architectures are predicted through the characterization of two-cell interactions," Proc. Natl. Acad. Sci. U. S. A. **111**, 6521 (2014).
[15] R. B. Bernstein and R. D. Levine, "Entropy and chemical change. I. Characterization of product (and reactant) energy distributions in reactive molecular collisions: Information and entropy deficiency," J. Chem. Phys. **57**, 434–449 (1972).
[16] R. D. Levine and R. B. Bernstein, "Energy disposal and energy consumption in elementary chemical reactions. Information theoretic approach," Acc. Chem. Res. **7**, 393–400 (1974).
[17] R. D. Levine and C. E. Wulfman, "On the group-theoretical formulation for the time evolution of stochastic processes," Physica A **141**, 489 (1987).
[18] J. L. Kinsey, "Microscopic reversibility for rates of chemical reactions carried out with partial resolution of the product and reactant states," J. Chem. Phys. **54**, 1206–1217 (1971).
[19] R. D. Levine, "Addressing the challenge of molecular change: An interim report," Annu. Rev. Phys. Chem. **69**, 1–21 (2018).
[20] J. von Neumann, *Mathematical Foundations of Quantum Mechanics* (Princeton University Press, Princeton, 1955).
[21] E. C. Kemble, "The quantum-mechanical basis of statistical mechanics," Phys. Rev. **56**, 1146 (1939).
[22] W. M. Elsasser, "On quantum measurements and the role of the uncertainty relations in statistical mechanics," Phys. Rev. **52**, 987 (1937).
[23] U. Fano, "Description of states in quantum mechanics by density matrix and operator techniques," Rev. Mod. Phys. **29**, 74 (1957).
[24] J. Wei and E. Norman, "On global representations of the solutions of linear differential equations as a product of exponentials," Proc. Am. Math. Soc. **15**, 327–334 (1964).
[25] Z. Bacić and J. C. Light, "Highly excited vibrational levels of 'floppy' triatomic molecules: A discrete variable representation—Distributed Gaussian basis approach," J. Chem. Phys. **85**, 4594 (1986).
[26] J. C. Light and T. Carrington, Jr., "Discrete-variable representations and their utilization," in *Advances in Chemical Physics*, edited by I. Prigogine and S. A. Rice (Wiley, New York, 2000), Vol. 114, p. 263.

[27]R. Kosloff, "Time-dependent quantum-mechanical methods for molecular dynamics," J. Phys. Chem. **92**, 2087 (1988).
[28]E. J. Heller, "Time-dependent approach to semiclassical dynamics," J. Chem. Phys. **62**, 1544 (1975).
[29]G. H. Golub and C. F. V. Loan, *Matrix Computations*, 3rd ed. (John Hopkins University Press, Baltimore, 1996).
[30]R. D. Levine, "Thermodynamic functions for state-selected chemical reactions," Chem. Phys. Lett. **39**, 205 (1976).
[31]K. Komarova, H. Gattuso, R. D. Levine, and F. Remacle, "Quantum device emulates the dynamics of two coupled oscillators," J. Phys. Chem. Lett. **11**, 6990 (2020).
[32]Y. Alhassid and R. D. Levine, "Connection between the maximal entropy and the scattering theoretic analyses of collision processes," Phys. Rev. A **18**, 89 (1978).
[33]M. Nielsen and I. Chuang, *Quantum Computation and Quantum Information*, 10th Anniversary ed. (Cambridge University Press, New York, USA, 2010).
[34]J. Paldus, "Group theoretical approach to the configuration interaction and perturbation theory calculations for atomic and molecular systems," J. Chem. Phys. **61**, 5321 (1974).
[35]J. Hinze, *The Unitary Group for the Evaluation of Electronic Energy Matrix Elements* (Springer-Verlag Berlin, Heidelberg, 1981).
[36]R. Schneider and W. Domcke, "S_1-S_2 conical intersection and ultrafast S2 → S1 internal conversion in pyrazine," Chem. Phys. Lett. **150**, 235 (1988).
[37]N. Agmon, Y. Alhassid, and R. D. Levine, "An algorithm for finding the distribution of maximal entropy," J. Comput. Phys. **30**, 250 (1979).
[38]H. Köppel, W. Domcke, and L. S. Cederbaum, "Multimode molecular dynamics beyond the Born–Oppenheimer approximation," in *Advances in Chemical Physics*, edited by I. Prigogine and S. A. Rice (Wiley, New York, 1984), Vol. 57, p. 59.
[39]Y. Su, D. Chen, C. Lausted, D. Yuan, J. Choi, C. Dai, V. Voillet, K. Scherler, P. Troisch, V. R. Duvvuri, P. Baloni, G. Qin, B. Smith, S. Kornilov, C. Rostomily, A. Xu, J. Li, S. Dong, A. Rothchild, J. Zhou, K. Murray, R. Edmark, S. Hong, L. Jones, Y. Zhou, R. Roper, S. Mackay, D. S. O'Mahony, C. R. Dale, J. A. Wallick, H. A. Algren, Z. A. Michael, A. Magis, W. Wei, N. D. Price, S. Huang, N. Subramanian, K. Wang, J. Hadlock, L. Hood, A. Aderem, J. A. Bluestone, L. L. Lanier, P. Greenberg, R. Gottardo, M. M. Davis, J. D. Goldman, and J. R. Heath, "Multiomic immunophenotyping of COVID-19 patients reveals early infection trajectories," bioRxiv:10.1101/2020.07.27.224063.